

Face-LLaVA: Facial Expression and Attribute Understanding through Instruction Tuning

Ashutosh Chaubey Xulang Guan Mohammad Soleymani
Institute for Creative Technologies, University of Southern California
Los Angeles, California, USA

{achaubey, xulanggu}@usc.edu, soleymani@ict.usc.edu

Abstract

The human face plays a central role in social communication, necessitating the use of performant computer vision tools for human-centered applications. We propose Face-LLaVA, a multimodal large language model for face-centered, in-context learning, including facial expression and attribute recognition. Additionally, Face-LLaVA is able to generate natural language descriptions that can be used for reasoning. Leveraging existing visual databases, we first developed FaceInstruct-1M, a face-centered database for instruction tuning MLLMs for face processing. We then developed a novel face-specific visual encoder powered by Face-Region Guided Cross-Attention that integrates face geometry with local visual features. We evaluated the proposed method across nine different datasets and five different face processing tasks, including facial expression recognition, action unit detection, facial attribute detection, age estimation and deepfake detection. Face-LLaVA achieves superior results compared to existing open-source MLLMs and competitive performance compared to commercial solutions. Our model output also receives a higher reasoning rating by GPT under a zero-shot setting across all the tasks. Both our dataset and model will be released at <https://face-llava.github.io/> to support future advancements in social AI and foundational vision-language research.

1. Introduction

The human face serves as a fundamental conduit for social communication. Hence, face analysis including facial expression recognition [73], action unit (AU) detection [92], facial attribute detection [94], age estimation [2] has received considerable attention. These tasks have a plethora of applications such as human-computer interaction [61], social behavior assessment [51], e-learning [20] and surveillance [50], among others.

Existing face analysis approaches suffer from two ma-

jor limitations: (i) they are developed for specific tasks such as expression recognition [7, 79] or attribute detection [42, 45], limiting their generalizability; and (ii) they primarily output labels without natural language description for their predictions. The ability to use natural language to describe predictions is crucial for critical applications such as healthcare and surveillance [11, 74].

To address the first limitation, recent advances have focused on developing generalist face models capable of handling multiple tasks [6, 54]. However, these models still lack a natural language interface, as they do not provide any insight into their decision-making process. The recent advent of Multimodal Large Language Models (MLLMs) such as LLaVA [28, 39, 86] has led to the application of such models for specific visual processing tasks, including face processing. EmoVIT [76] uses instruction tuning to enhance visual emotion understanding of large vision and language models. Emotion-LLaMA [8] uses an MLLM to take audio, video and text inputs to generate a description of emotional responses and reasoning in a given video. Foteinopoulou et al. [12] investigate the deepfake detection and reasoning capabilities of existing large language models (LLMs). However, these approaches are task-specific and involve prediction using background information or audio. More recently, MLLMs have been adapted for face processing, e.g., FABA [34] and VL-FAU [15] attempting to bridge the gap by leveraging powerful visual encoders and LLMs reasoning capabilities. However, the capabilities of these methods are limited to analyzing static images, solely focusing on facial expression analysis.

In this paper, we propose Face-LLaVA, a generalist MLLM that can perform perception with reasoning on different face analysis tasks. Fig. 1 shows the interaction of a user with our model. Note that given a video or an image, our model can recognize facial expressions, facial action units, age, and facial attributes and identify face forgery (see Fig. 2). This advancement paves the way for developing general-purpose AI-driven social agents with enhanced facial reasoning capabilities, making them more applicable

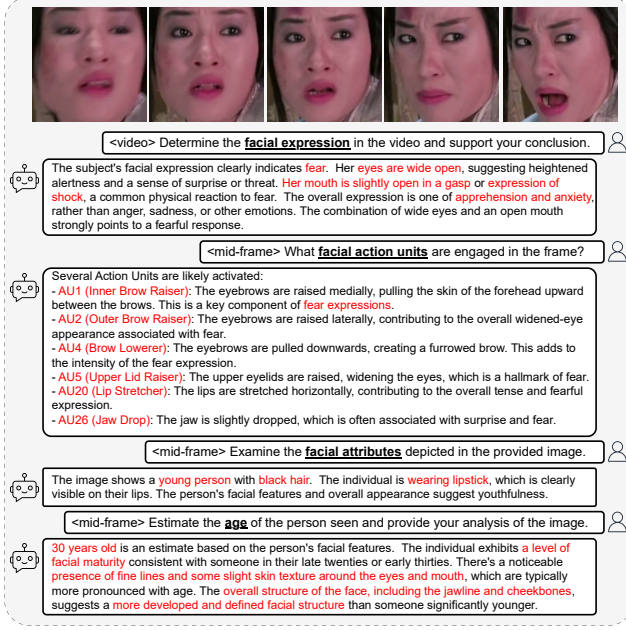


Figure 1. A sample conversation with Face-LLaVA highlighting different face tasks that our model is capable of performing.

to real-world scenarios.

Training an MLLM for face analysis requires a vast amount of instruction-tuning data covering different tasks. However, existing instruction-tuning datasets [8, 34, 36] for related tasks are relatively small, task-specific, and often limited to either images or videos (see Tab. 1). To address this limitation, we introduce *FaceInstruct-1M*, a large-scale face-specific dataset comprising one million samples, including around 850k images and 120 hours of video data, annotated with task-specific instructions and descriptions across five distinct face analysis tasks. Furthermore, as the dataset is automatically generated, we employ a GPT-4o [67]-assisted evaluation and filtering process to ensure high-quality data for fine-tuning the MLLM.

General-purpose vision encoders used in MLLMs, such as CLIP [55] and LanguageBind [93], are not designed to extract face-specific features such as facial landmarks, which are crucial for fine-grained face analysis. To address this, we propose a novel architecture that is specifically designed for face processing to enhance its performance. Unlike previous approaches [34], our method is more efficient in utilizing the LLM’s context window and is generalizable to both images and videos. Specifically, we introduce a *face-region landmark projector*, which maps face expert (landmark) features to face-region tokens and refines visual features via cross-attention with the extracted visual tokens.

We conduct extensive experiments on nine datasets spanning five different face analysis tasks, demonstrating that our method outperforms existing MLLMs across all benchmarks in a zero-shot setting and achieves performance com-

petitive with supervised task-specific approaches. To further assess the reasoning capabilities of our model, we conduct automatic GPT-based evaluations comparing our approach against recent MLLMs and showcasing its superior generative and captioning capabilities.

In summary, the key contributions of this work are as follows. (i) We introduce *FaceInstruct-1M*, a large-scale face analysis dataset comprising one million instruction-tuning samples, including both images and videos. The dataset spans five key face-related tasks: expression recognition, action unit (AU) detection, attribute detection, age estimation, and deepfake detection. (ii) We propose *Face-LLaVA*, a multimodal large language model architecture for face analysis that incorporates face landmark features using a face-region projector and face-region-guided cross-attention, enabling effective instruction tuning for face processing tasks. (iii) Through extensive experiments, we demonstrate that our approach outperforms existing MLLMs in a zero-shot setting on nine datasets across five face analysis tasks, achieving superior performance on both traditional benchmarks and GPT-assisted evaluations of generated responses. Additionally, we show that our method achieves competitive performance with supervised task-specific techniques across all tasks.

FaceInstruct-1M and *Face-LLaVA* model weights will be released at <https://face-llava.github.io/> upon acceptance.

2. Related Works

2.1. Traditional face analysis

Extensive research has been conducted on individual face analysis tasks, including expression recognition [7, 64, 70, 75, 79, 80, 84, 85], action unit detection [33, 43, 59, 65], age estimation [2, 13, 62], attribute detection [42, 45, 58], and deepfake detection [1, 9, 52]. However, the research focus is gradually shifting towards developing generalist face analysis models [48, 53, 54] and learning robust facial representations [6, 60, 91]. Faceptor [54] builds upon FaRL [91] and SWINFace [53] by introducing a single encoder with a dual-decoder transformer to handle multiple face analysis tasks. MARLIN [6] and PrefAce [19] leverage self-supervised learning on video data using masked autoencoders (MAE) [16, 69] to learn robust facial representations. PCL [41] employs a pose-disentangled decoder for contrastive learning, generating robust pose and appearance features for face analysis. Building on these advancements, our work introduces a generalist face analysis model that extends beyond face perception by incorporating reasoning over its predictions. This enhances interpretability and enables more detailed and context-aware facial analyses.

2.2. Face analysis using instruction tuning

Multimodal LLMs enhance reasoning and analysis on visual and other inputs by leveraging the extensive knowledge encoded in LLMs [37, 39, 68, 81, 86]. These models require large-scale instruction-tuning datasets consisting of a visual (or other modality) input, an instruction, and corresponding responses [39, 86]. The use of MLLMs for face analysis remains limited due to the scarcity of large-scale instruction-tuning data. Most traditional face analysis datasets [22, 42, 46, 47, 56, 57] provide only categorical or numerical labels (see Tab. 1). While instruction or description datasets exist for general emotion recognition, they primarily rely on background context and audio rather than facial cues alone [8, 36, 40, 76]. FABAInstruct [34] is a face-specific dataset but is limited to still images and affective behavior analysis. In contrast, we introduce *FaceInstruct-1M*, a large-scale instruction-tuning dataset explicitly designed for face analysis across multiple face-related tasks.

While prior research has explored reasoning with large VLMs for face-related tasks [8, 12, 76], dedicated efforts toward comprehensive face-specific reasoning remain scarce. AU-LLAVA [18] utilizes an LLM for AU detection and intensity estimation, yet its outputs are restricted to categorical or numerical predictions without reasoning. VL-FAU [15] introduces a vision-language framework for interpretable AU detection, while EmoLA [34] integrates landmark prior tokens with visual embeddings to facilitate facial affective behavior analysis with reasoning. Similarly, EMO-LLaMA [77] employs a face-information mining module to enhance facial feature encoding, demonstrating both reasoning and conversational capabilities.

More recently, Face-MLLM [63] employed Gemini to automatically annotate face images in the Laion-Face [90] dataset for instruction tuning, although its focus remains solely on perception rather than reasoning over model predictions, and it depends heavily on Gemini’s face analysis capabilities to build its dataset. Similarly, FaVChat [88] leverages existing face video datasets for instruction tuning; however, due to significant class imbalances in attributes such as emotion in datasets like CelebV-HQ [94], the overall dataset becomes imbalanced. Moreover, both approaches do not generalize well to both images and videos and often include background information that might cause model hallucinations. In contrast, Face-LLaVA handles both images and videos, relies on standard, well-established datasets for instruction data construction, and is tailored specifically for videos, thereby reducing the likelihood of hallucinations stemming from background content.

3. FaceInstruct-1M

In this section, we introduce *FaceInstruct-1M*, a dataset designed for instruction-tuning MLLMs on face-centric tasks.

Dataset	Face Spec.	Modality		Number of Samples					Anno.	
		Img.	Vid.	Expr.	AU	Attr.	Age	DF.		Tot.
RAF-DB [31]	✓	✓	✗	30k	-	-	-	-	30k	C
AffectNet [47]	✓	✓	✗	440k	-	-	-	-	440k	C
DFEW [22]	✓	✗	✓	16k	-	-	-	-	16k	C
FERV39K [72]	✓	✗	✓	39k	-	-	-	-	39k	C
DISFA [46]	✓	✓	✗	-	140k	-	-	-	140k	C
BP4D [83]	✓	✓	✗	-	150k	-	-	-	150k	C
AffWild2 [26]	✓	✓	✗	2.6M	2.6M	-	-	-	2.6M	C+N
CelebA [42]	✓	✓	✗	-	-	200k	-	-	200k	C
MORPH II [56]	✓	✓	✗	-	-	-	50k	-	50k	N
UTK Face [87]	✓	✓	✗	-	-	-	20k	-	20k	N
FF++ [57]	✓	✗	✓	-	-	-	-	5k	5k	C
Fake-AVC [25]	✓	✗	✓	-	-	-	-	20k	20k	C
EMER [36]	✗	✗	✓	450	-	-	-	-	450	D
MAFW [40]	✗	✗	✓	10k	-	-	-	-	10k	C+SD
EmoVIT [76]	✗	✗	✓	1.6k	-	-	-	-	1.6k	I+D
MERR [8]	✗	✗	✓	30k	-	-	-	-	30k	I+D
FABA Instr. [34]	✓	✓	✗	20k	20k	-	-	-	20k	I+D
Face-Instruct-1M	✓	✓	✓	350k	290k	200k	70k	95k	1M	I+D

Table 1. Comparison of the proposed *FaceInstruct-1M* dataset with various annotated datasets of face-related tasks. C:category, SD:short description, I:instruction, D:description, N:number (regression), DF.: deepfake detection, Face Spec.: Face-Specific., AU: action unit.

As shown in Tab. 1, it provides instructions and descriptions for expression recognition, AU detection, deepfake detection, attribute detection, and age estimation. Unlike existing datasets [22, 42, 46, 57, 72] that focus on individual tasks, *FaceInstruct-1M* spans multiple domains. While prior instruction-tuning [8, 76] and captioning [36, 40] datasets annotate entire images/videos, including background context and audio, ours is specifically curated for face analysis. Though FABA-Instruct [34] is face-specific, it is limited to images, has fewer samples, and covers only two tasks. To the best of our knowledge, *FaceInstruct-1M* is the first large-scale instruction-tuning dataset for face analysis, spanning multiple tasks with both images and videos.

3.1. Annotation Pipeline

FaceInstruct-1M is constructed using images, videos, and annotations from existing task-specific datasets as men-

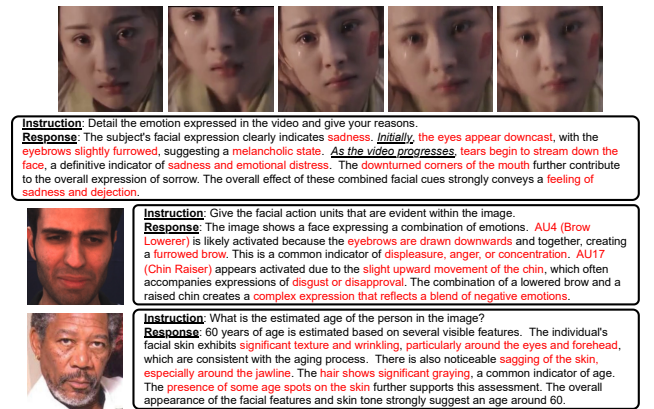


Figure 2. *FaceInstruct-1M* dataset samples for different tasks.

Task	Datasets	Mean GPT Rating (1-10)			Overall
		Label Acc.	Desc.-Vid. Consistency	Desc.-Lab. Consistency	
FaceInstruct-1M					
Expression	DFEW [22], MAFW [40], FERV39k [72] Crema-D [24], AffectNet [47], RAF-DB [31]	8.81	8.74	8.79	8.71
AU	DISFA [46], BP4D [83]	8.17	8.23	7.62	7.99
Attribute	CelebA [42]	8.79	8.75	8.52	8.69
Age	MORPH II [56], UTK Face [87]	8.63	7.92	7.98	7.99
Deepfake*	FF++ [57], Fake AV Celeb [25]	8.84	8.13	8.60	8.20
FABAIInstruct [34]					
Expression	AffectNet [47]	8.79	6.44	6.32	6.22

Table 2. Datasets used to construct the *FaceInstruct-1M* and GPT [67] ratings for different aspects of the data. Ratings for FABAIInstruct [34] are calculated as a reference. *For deepfake detection, we annotate a set of real videos from DFEW [22], MAFW [40], FERV39k [72] as control samples.

tioned in Tab. 2 (see Appendix D for details). Since, we are only interested in face, we apply some data preprocessing to crop the faces in videos and only use such samples in which there is a single subject present during the entire duration of the video (Appendix E.1 for details).

We found that existing manual annotations in various face datasets, despite being categorical or containing minimal information, can significantly aid in guiding the automatic generation of descriptions that align with the data (Appendix E.5). To generate video descriptions for specific tasks, we provide the face video and its categorical label, along with carefully designed annotation instructions, to Gemini 1.5 Flash [66]. Gemini was selected among open and commercial models due to its superior performance, faster inference, higher rate limits and low cost. As an example, our annotation instruction for the facial expression recognition task follows this structure: ‘*The given video has ... emotion. Your task is to reason why the emotion is tagged as Focus specifically on the facial expression of the subject in the video and describe how it varies. ... {output format instructions}*’. Following FABAIInstruct [34], we associate each description and video/image pair with a corresponding set of instructions for instruction-tuning. To achieve this, we carefully curate a collection of 100 hand-crafted instructions for each task and randomly pair them with the generated descriptions. Refer to Appendix E for more details.

3.2. Dataset Rating and Filtering

Tab. 2 lists the constituent datasets of *FaceInstruct-1M*, where we observe that some datasets [22, 40, 42, 72] are not exclusively face-specific and therefore include background context and audio. Consequently, the manual annotations in these datasets may be influenced by these additional contextual elements rather than solely by facial expressions or facial features. Furthermore, since our annotations are generated using an LLM, it is crucial to perform a sanity check and apply filtering to ensure high data quality.

We employ a GPT-assisted rating pipeline for data filter-

ing, which takes the video/image, manually annotated label and Gemini-generated description and rate them based on instructions. We use GPT-4o mini [67] for rating according to (i) accuracy of the manually annotated label w.r.t. the face video, (ii) consistency of the generated description with the face video, (iii) consistency of the generated description with the manually annotated label, and (iv) overall quality of the sample based on resolution, visibility of the face, etc. Tab. 2 summarizes the ratings by GPT-4o-mini [67]. To calibrate the ratings, we also perform GPT-evaluation of FABAIInstruct [34]. *FaceInstruct-1M* consistently achieves high ratings from GPT, demonstrating high data quality. Samples with an overall rating less than or equal to six are removed from *FaceInstruct-1M* for training, resulting in the removal of roughly 7% of the dataset.

3.3. Qualitative analysis

Fig. 2 presents samples from the *FaceInstruct-1M* dataset across different tasks. Notably, for video inputs, the descriptions capture subtle variations in various facial attributes and justify the responses to the given instructions based on these observations. It is also important to highlight that the dataset encompasses tasks reliant on muscle movements (e.g., expression recognition, AU detection, and deepfake detection), facial attributes (including age), and overall video quality (deepfake detection). This diverse coverage makes *FaceInstruct-1M* well-suited for learning a broad range of facial features across different categories.

3.4. Evaluation

Since an MLLM trained on our dataset generates natural language, its evaluation must consider both (i) metrics for face analysis, such as average recall or accuracy (Appendix F.3), and (ii) the reasoning capabilities w.r.t. instructions. Similar to FABAIInstruct [34], we assess traditional metrics using synonym matching (refer Appendix F.1) for expression recognition, attribute detection, and deepfake detection, while for AU detection and age estimation, we extract numerical values directly from the generated text. To ensure accuracy, negative statements are removed before synonym matching or string parsing. For tasks requiring a single prediction label, majority voting is applied. Once categorical or numerical labels are extracted from the descriptions, task-specific metrics are calculated.

For evaluating the reasoning capabilities of MLLMs on face tasks, traditional text generation metrics such as BLEU [49] or ROUGE [38] can be used to match the generated description with the ground truth. However, such metrics are based on crude n-gram matches rather than in-depth semantic analysis of the generated description. Hence, we evaluate the reasoning capabilities using GPT4o-mini [67] on the following aspects similar to Sec. 3.2 - (i) consistency or overlap of the given reasoning with video, (ii) consistency

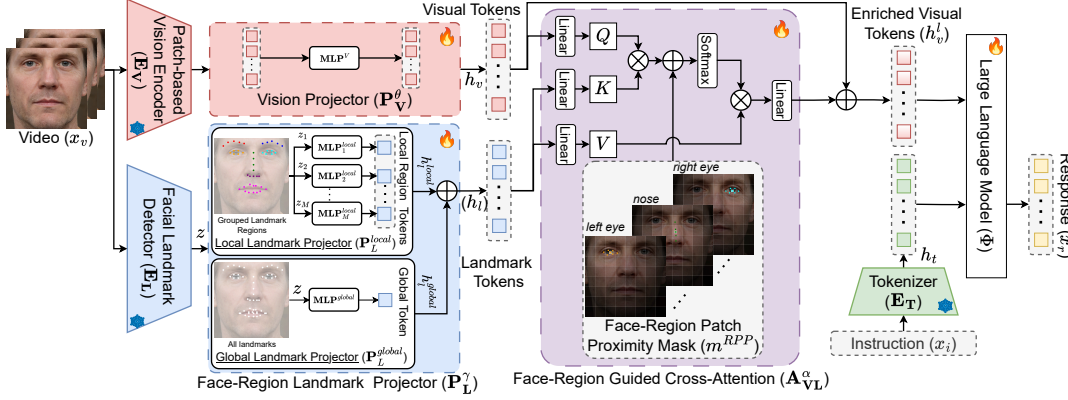


Figure 3. Proposed Face-LLaVA architecture. We group landmark points into different face regions and project them through a face-region landmark projector. The visual tokens are enriched by the landmark tokens through cross-attention and then passed as input to the LLM.

or overlap of the given reasoning with ground truth label, and (iii) overall completeness of the reasoning to support the ground truth label w.r.t the video.

Furthermore, we construct a small test set for *FaceInstruct-1M* consisting of 500 samples for each of the five tasks using DFEW [22], DISFA [46], CelebA [42], UTKFace [87] and FaceForensics++ [57]. We start with the samples that are top-rated by GPT and then refine the set so that the class distribution of test samples for each task match the original dataset. Such a small and carefully crafted set also enables other holistic evaluations of reasoning, such as human evaluation, which is expensive.

4. Face-LLaVA

Fig. 3 illustrates the Face-LLaVA architecture for instruction-tuning on face images and videos. Similar to prior MLLMs [37, 39], it consists of a patch-based vision encoder E_V to encode input image (or video), a tokenizer E_T to encode the text instruction and a large language model decoder Φ to generate responses according to the instruction x_i . Inspired by Lin et al. [93], we use LanguageBind [93] vision encoders for video and image and learn a joint vision projector P_V^θ from the visual token space to the language token space. Specifically, given a visual input x_v , we get visual tokens $h_v \in \mathbb{R}^{T \times N \times d}$ as follows,

$$h_v = P_V^\theta(E_V(x_v)) \quad (1)$$

where T is the number of video frames (1 for images), N is the number of visual tokens from the patch-based vision encoder E_V (256 for LanguageBind), and d is the dimensionality of hidden representation of the LLM.

Since we are dealing with faces, the visual information should also incorporate features specifically important for face processing which can be obtained from a *face-expert* model E_L . In Face-LLaVA, we use a landmark detector as our *face-expert* model to extract face-specific features from the visual input x_v . We also experimented with a face-

parsing model as the expert, but that led to extra computing due to pixel-wise information and no returns (see Sec. 5.4). Formally, we obtain the normalized 2-D landmark coordinates, $z = E_L(x_v)$ where $z \in \mathbb{R}^{T \times L \times 2}$. These expert features are then fed to the proposed novel *Face-Region Landmark Projector* and *Face-Region Guided Cross-Attention* modules.

4.1. Face-Region Landmark Projector (FRLP)

To project the facial landmark features to the token space, one can simply flatten the L facial landmarks into the LLM’s d -dimensional token space by projection [34]. However, this maps the entire face landmark features into a single token without preserving information about what individual landmark points mean. Moreover, for a lot of complex face-perception tasks, humans tend to look at a group of facial muscles or regions, such as eyes or lips, to make informed decisions. For example, to detect an expression of disgust, visual features around the nose to capture wrinkling are important. Therefore, we propose a *Face-region Landmark Projector* to group landmarks into different face regions and then project them into individual face-region tokens through separate MLPs. Specifically, we use two sub-modules to tokenize the landmark features.

The *local landmark projector* P_L^{local} generates M tokens each corresponding to a separate face-region,

$$h_l^{local} = \{\text{MLP}_i^{local}(z_i) \mid i \in \{1 \dots M\}\} \quad (2)$$

where $z_i \in \mathbb{R}^{T \times L_i \times 2}$ are the L_i 2-D landmark points corresponding to the i^{th} face region. We use a total of 9 landmark groups corresponding to the following face regions - *face boundary, left/right eye, left/right brow, nose, nostril, lips and teeth*.

Similar to EmoLA [34], we also project all the L landmark points through a *global landmark projector* P_L^{global} to get a single global landmark token for each frame which can capture the overall facial structure and dynamics beyond in-

dividual regions.

$$h_l^{global} = \mathbf{MLP}^{global}(z) \quad (3)$$

and the final landmark tokens h_l are given by,

$$h_l = h_l^{global} + h_l^{local} \quad (4)$$

where the global token h_l^{global} is broadcasted in the token dimension. By combining the local region and the global landmark tokens, our approach ensures that both local and holistic facial features are effectively modeled. To keep the extra compute to a minimum, we use single-layer MLPs for all the landmark projections.

4.2. Face-Region Guided Cross-Attention(FRGCA)

We propose to use the landmark tokens h_l generated by the FRLP module via cross-attention with the visual tokens h_v . Such an architecture poses two benefits - (i) using cross-attention enables weighing visual tokens that are closer to salient face regions and are highly likely to be used by the downstream face processing tasks, and (ii) as opposed to EmoLA [34], the M landmark tokens per frame do not have to be appended to the visual tokens and passed as input to the LLM thus saving the LLM’s context window. Formally, we obtain the key ($K \in \mathbb{R}^{M \times d_{attn}}$) and value ($V \in \mathbb{R}^{M \times d_{attn}}$) vectors using h_l , and the query ($Q \in \mathbb{R}^{N \times d_{attn}}$) vector using h_v by passing through separate linear layers. Note that we have dropped the time dimension T for simplicity.

To further enforce the attention weights on face regions, we compute a *face-region patch proximity* (RPP) mask, which is inversely proportional to the pairwise 2-D distances between the centroids of the visual patches used as inputs by \mathbf{E}_V and the centroids of the different face regions as shown in Figure Fig. 3. Mathematically, the elements of the mask m^{RPP} are given by

$$m_{ji}^{RPP} = -||centroid(z_i) - centroid(h_{v,j})||_2 \quad (5)$$

where $centroid(z_i)$ is the centroid of i^{th} face region, $centroid(h_{v,j})$ is the centroid of the j^{th} visual patch associated with the visual token $h_{v,j}$, and $m^{RPP} \in \mathbb{R}^{N \times M}$.

The RPP mask is used to guide the attention weights before the softmax layer. The entire FRGCA module \mathbf{A}_{VL}^α can be summarized as,

$$h_v^l = \text{Linear} \left(\text{Softmax} \left(\frac{QK^T}{\sqrt{d_{attn}}} + m^{RPP} \right) V \right) + h_v \quad (6)$$

4.3. Training

We train the Face-LLaVA model in multiple stages so that the visual and landmark tokens can be aligned with the language tokens. We initialize the vision encoder(\mathbf{E}_V), vision

projector (\mathbf{P}_V^θ), tokenizer (\mathbf{E}_T) and the LLM (Φ) from the pretrained weights of Video-LLaVA [37]. For landmark detection, we use pretrained weights from FAN [5].

Face-Region Pretraining. In this stage, we only train the FRLP module \mathbf{P}_L^γ and the FRGCA module \mathbf{A}_{VL}^α and keep all the other weights frozen, hence, the trainable parameters are given by $\Theta = \{\gamma, \alpha\}$. This ensures that the newly initialized modules generating landmarks tokens get aligned with the visual and the language tokens generated by \mathbf{P}_V^θ and \mathbf{E}_T respectively.

Finetuning. In this stage, we train the vision projector \mathbf{P}_V^θ and the LLM model Φ along with \mathbf{P}_L^γ and \mathbf{A}_{VL}^α with a lower learning rate. This stage jointly finetunes the entire model to further improve the instruction following capabilities of the model. The trainable parameters here are given by $\Theta = \{\gamma, \alpha, \theta, \phi\}$. Note that since we have a good number of training samples in *FaceInstruct-1M*, we train all the parameters ϕ of the LLM rather than using LoRA [17].

For both stages, the model is trained in an autoregressive fashion by maximizing the likelihood of the response x_r :

$$P(x_r|h_v^l, h_t) = \prod_{i=1}^{\mathcal{L}} P_{\Theta}(x_r^i|h_v^l, h_t, x_r^{[1:i-1]}) \quad (7)$$

where x_r^i is the i^{th} response token, \mathcal{L} is the length of the response x_r , and $x_r^{[1:i-1]}$ are the response tokens generated before the i^{th} token. Learning rates for the pretraining and finetuning stages are 1e-4 and 2e-5 respectively, and all the models are trained for one epoch (see Appendix G for details).

5. Experiments

5.1. Datasets and Evaluation Protocol

Perception. We perform extensive evaluations of the proposed approach on nine benchmarks including DFEW [22], Crema-D [24], and RAF-DB [31] for facial expression recognition; DISFA [46] and BP4D [83] for action unit detection; FaceForensics++ [57] for deepfake detection; MORPH II [56] and UTK Face [87] for age estimation and CelebA [42] for facial attribute detection (Appendices D and F.3 for details). Since these datasets are also used to construct the *FaceInstruct-1M* dataset, we report performance on these datasets in the following two settings. In the *zero-shot* setting, we remove the entire task-specific dataset from *FaceInstruct-1M* for tuning our model, and in the *fine-tuned* setting we finetune the *zero-shot* model according to the official splits or training protocol of the benchmark (Appendix F.3).

Reasoning. As mentioned in Sec. 3.4, we perform reasoning evaluation using GPT4o-mini [67] on *FaceInstruct-1M test* set consisting of 500 samples per task. We do not use the existing EMER [36] benchmark for reasoning evalua-

DFEW [22]			Crema-D [24]			RAF-DB [31]	
Method	UAR \uparrow	WAR \uparrow	Method	UAR \uparrow	WAR \uparrow	Method	Acc. \uparrow
<i>Closed-source models</i>							
GPT4o-mini [67]	0.426	0.518	GPT4o-mini [67]	0.410	0.486	GPT4o-mini [67]	0.758
Gemini-1.5F [66]	0.433	0.481	Gemini-1.5F [66]	0.465	0.635	Gemini-1.5F [66]	0.685
<i>Zero-shot</i>							
Vid.LLaMA 3 [81]	0.286	0.305	Vid.LLaMA 3 [81]	0.397	0.546	Vid.LLaMA 3 [81]	0.671
Qwen 2.5 [68]	0.293	0.399	Qwen 2.5 [68]	0.395	0.566	Qwen 2.5 [68]	0.526
Vid.-LLaVA [37]	0.220	0.326	Vid.-LLaVA [37]	0.367	0.557	Vid.-LLaVA [37]	0.545
LLaVA-Vid. [86]	0.375	0.498	LLaVA-Vid. [86]	0.478	0.618	LLaVA-OV [28]	0.700
EmoLA* [34]	0.346	0.449	EmoLA* [34]	0.431	0.618	EmoLA [34]	0.741
Emotion LLaMA [†] [8]	0.456	0.594	Emotion LLaMA [8]	0.225	0.308		
Emotion LLaMA [‡] [8]	0.302	0.378					
Face-LLaVA (Ours)	0.469	0.564	Face-LLaVA (Ours)	0.582	0.681	Face-LLaVA (Ours)	0.780
<i>Fine-tuned</i>							
EC-STFL [22]	0.454	0.565	Lei et al. [27]	0.645	0.648	RUL [84]	0.890
Former-DFER [89]	0.537	0.657	PTH-Net [30]	0.699	0.700	EAC [85]	0.909
GCA+IAL [29]	0.557	0.692	MAE-DFER [64]	0.773	0.774	TransFER [79]	0.909
M3DFEL [70]	0.561	0.693	MTL-ER* [82]	0.745	0.756	Xue et al. [80]	0.920
MAE-DFER [64]	0.634	0.744	MT-Former* [78]	0.793	0.807	POSTERv2 [44]	0.922
S2D [7]	0.618	0.760	MTCAE-DFER [75]	0.847	0.850	EmoLA [34]	0.921
EMO-LLaMA [77]	0.602	0.659					
Emotion-LLaMA [8]	0.642	0.771					
Face-LLaVA (Ours)	0.625	0.745	Face-LLaVA (Ours)	0.798	0.813	Face-LLaVA (Ours)	0.921

Table 3. Comparison of the proposed approach with recent MLLMs and supervised techniques for emotion recognition on the DFEW [22], Crema-D [24] and RAF-DB [31] dataset. *:Only using middle video frame, †: Results taken from the paper [8], ‡: Results computed after running inference code on face-cropped video.

Age Estimation (MAE \downarrow)			Face Attribute (mAcc. \uparrow)		DeepFake Det. (Acc. \uparrow)	
Method	M [56]	U [87]	Method	CA [42]	Method	FF [57]
<i>Closed-source models</i>						
GPT4o-m [67]	4.09	5.04	GPT4o-m [67]	0.780	GPT4o-m [67]	0.807
Gem.-1.5F [66]	4.78	6.13	Gem.-1.5F [66]	0.814	Gem.-1.5F [66]	0.770
<i>Zero-shot</i>						
V-LLaMA3 [81]	6.98	6.91	V-LLaMA3 [81]	0.813	V-LLaMA3 [81]	0.793
Qwen 2.5 [68]	6.09	5.25	Qwen 2.5 [68]	0.786	Qwen 2.5 [68]	0.653
V-LLaVA [37]	6.75	5.89	V-LLaVA [37]	0.795	V-LLaVA [37]	0.697
LLaVA-OV [28]	6.33	6.87	LLaVA-OV [28]	0.805	LLaVA-V [86]	0.751
Face-LLaVA	3.34	4.89	Face-LLaVA	0.868	Face-LLaVA	0.845
<i>Fine-tuned</i>						
PML [10]	2.15	-	Liu et al. [42]	0.873	MesoNet [1]	0.705
Berg et al. [4]	-	4.55	MOON [58]	0.909	Xception [9]	0.869
DLDL-v2 [14]	1.97	4.42	SwinFace [53]	0.913	MARLIN [6]	0.894
MWR [62]	2.00	4.37	Faceptor [54]	0.914	M2TR [71]	0.929
Faceptor [54]	1.96	4.10	DMM-CNN [45]	0.917	F3-Net [52]	0.930
Face-LLaVA	2.02	4.06	Face-LLaVA	0.901	Face-LLaVA	0.888

Table 5. Comparison of the proposed approach with recent MLLMs and supervised techniques on the age estimation, face attribute detection and deepfake detection tasks on different datasets [42, 56, 57, 87]. M: MORPH II [56], U: UTKFace [87], CA: CelebA [42], FF: FaceForensics++ [57].

tion because we want to assess the reasoning based on facial expressions and not the background context or audio.

5.2. Evaluation on traditional tasks

We assess Face-LLaVA against multiple baselines under both *zero-shot* and *fine-tuned* settings, following the evaluation protocol detailed in Sec. 5.1. Unless otherwise, we apply the official inference code to face-cropped inputs for *zero-shot* baselines (Appendix G.2) and report the officially published results for *fine-tuned* baselines. Additionally, for GPT4o-mini [67] and Gemini 1.5 Flash [66], official APIs are used to perform batch inference.

Facial Expression Recognition. Tab. 3 summarizes the results of the proposed approach on FER compared to different baselines. Face-LLaVA outperforms almost all the baselines on all the benchmarks under a zero-shot setting.

Method	Average F1 \uparrow	
	DISFA [46]	BP4D [83]
<i>Closed-source models</i>		
GPT4o-mini [67]	0.429	0.496
Gemini-1.5F [66]	0.515	0.532
<i>Zero-shot</i>		
VideoLLaMA 3 [81]	0.374	0.458
Qwen 2.5 VL [68]	0.431	0.467
Video-LLaVA [37]	0.442	0.445
LLaVA-OneVision [28]	0.280	0.439
EmoLA [34]	0.418	0.407
Face-LLaVA (Ours)	0.553	0.495
<i>Fine-tuned</i>		
ATCM [21]	0.615	0.642
ReCoT [33]	0.626	0.648
KS [32]	0.628	
ME-GraphAU [43]	0.631	0.655
JAA-Net [59]	0.635	0.624
PIAP-DF [65]	0.638	0.641
VL-FAU [15]	0.665	0.658
AU-LLaVA [18]	0.525	0.603
EmoLA [34]	0.651	0.642
Face-LLaVA (Ours)	0.729	0.658

Table 4. Comparison of the proposed approach with recent MLLMs and supervised techniques on average F1 over the 8 AUs of DISFA [46] and 12 AUs of BP4D [83].

Emotion-LLaMA [8] achieves superior weighted average recall (WAR) compared to our approach, but it is important to note that it is a multimodal model using audio as well as background context to make its predictions. As reported in the table, if we remove the background context, the performance of Emotion-LLaMA deteriorates significantly. Moreover, Face-LLaVA achieves competitive performance compared to the baselines in a finetuned setting as well despite lacking any background and audio context for DFEW [22] and Crema-D [24] datasets. It is also important to note that, in contrast to other MLLM baselines [8, 34], our model for finetuned setting is still trained to provide descriptions rather than outputting a single categorical label.

AU Detection. Tab. 4 summarize the results for action unit detection on DISFA [46] and BP4D [83] datasets. Note that since BP4D and DISFA have a disjoint set of AU annotations, for training the model on a zero-shot setting, we augment *FaceInstruct-1M* with Gemini-1.5 Flash [66] annotated AffectNet [47] images. Hence, AU information is injected in the zero-shot training by the AffectNet samples and the dataset other than the benchmark dataset (BP4D/DISFA) on which we are reporting the numbers. Face-LLaVA outperforms all the zero-shot and fine-tuned baselines on average F1 scores on both datasets. On DISFA, we achieve a relative improvement of around 10% on the previous finetuned SOTA. Moreover, we achieve around 7% performance boost over Gemini-1.5 Flash [66], further showing the effectiveness of our model and training set.

Age Estimation, Attribute Detection, and Deepfake Detection. Tab. 5 contains the results of the proposed approach on Morph II [56], UTKFace [87], CelebA [42] and FaceForensics++ [57] benchmarks. Similar to AU detec-

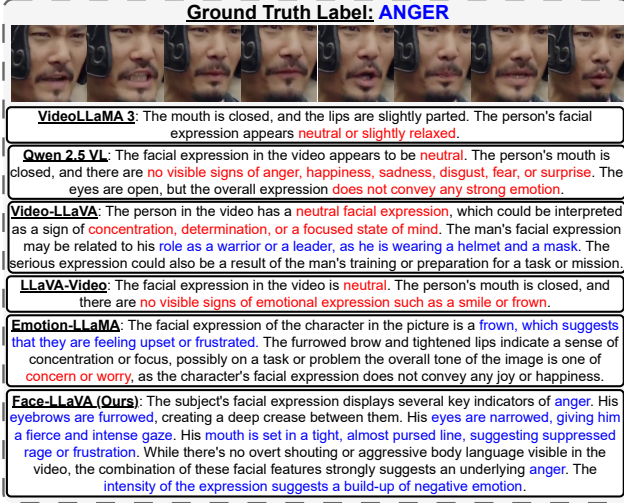


Figure 4. Comparison of Face-LLaVA with other MLLM baselines on the task of facial expression recognition. Red text indicates misaligned text and blue text indicates aligned/correct text according to the video and ground truth label.

tion, Face-LLaVA outperforms all the zero-shot baselines and achieves competitive performance with finetuning for age estimation and facial attribute detection benchmarks. It is notable to achieve competitive results in comparison to regression-based baselines for age estimation while using an MLLM. For attribute detection, due to the lack of large-scale supervised datasets, we annotate FFHQ [23] through Gemini-1.5 Flash without labels and use that to train Face-LLaVA for zero-shot performance comparison on CelebA [42] dataset. For deepfake detection, we report all the results on low-quality videos of FaceForensics++ [57]. All the zero-shot MLLM baselines, including GPT4o-mini and Gemini-1.5 Flash, achieve close to or worse than the baseline random accuracy of 80%. However, Face-LLaVA achieves significantly better accuracy in a zero-shot setting. The significant gap between the SOTA of deepfake detection [52] and Face-LLaVA in a fine-tuned setup can be attributed to the fact that the fine-tuned baselines use a higher number of frames per video while our model can only take eight frames per video.

5.3. Evaluation of reasoning

As mentioned in Sec. 3.4, we compare the reasoning capabilities of baselines with Face-LLaVA using GPT evaluation on the *FaceInstruct-1M* test set. Face-LLaVA achieves superior ratings compared to other MLLM baselines [28, 37, 68, 81]. Across all tasks, Face-LLaVA’s mean rating for completeness of reasoning is around 33% higher than the best baseline, with a mean rating of 7.60/10. Moreover, Face-LLaVA responses achieve higher mean ratings than the baselines on response-video consistency and response-GT consistency as well highlighting excellent vision language alignment and high accuracy. Detailed summary

of results can be found in Tab. 10 in Appendix C. Fig. 4 presents a comparison of reasoning generated by different MLLMs for facial expression recognition in a video.

5.4. Ablation Study

We evaluate the contribution of different modules in an ablation study and report zero-shot model performance on DFEW [22] using MAFW [40], FERV39k [40] and CremaD [24] for training. Our baseline model for this analysis is Video-LLaVA [37], which only uses the visual tokens h_v as input. We can clearly observe that using landmark tokens h_l (or h_l^{local}/h_l^{global}) similar to EmoLA [34] as inputs in addition to the visual tokens h_v , improves baseline performance but not as much as incorporating the landmark tokens using cross-attention with the visual tokens h_v . Moreover, using FRGCA, which incorporates masked attention through region-patch proximity mask m^{RPP} , leads to a larger performance gain than a simple cross-attention. Finally, to compare using landmarks as opposed to face-parse heatmaps, we encode the face-parse heatmaps through the visual encoder E_V and replace the landmark tokens for cross-attention with visual tokens. Face parse maps show competitive performance compared to FRLP+FRGCA, at an extra compute and memory cost for the face-parse tokens (same size as visual tokens h_v).

Model	Landmark Projector	Cross-Attention	Input tokens	DFEW [22]	
				UAR	WAR
Baseline	-	-	h_v	0.391	0.479
Baseline + Landmarks	only global	-	$h_v + h_l^{global}$	0.402	0.483
	only local	-	$h_v + h_l^{local}$	0.409	0.491
	FRLP	-	$h_v + h_l$	0.410	0.491
	only global	simple	h_v^{global}	0.401	0.483
	only local	simple	h_v^{local}	0.409	0.494
	FRLP	simple	h_v^l	0.416	0.512
	only local	FRGCA	h_v^{local}	0.412	0.511
Baseline + Face Parsing	-	simple	h_v^p	0.424	0.520

Table 6. Ablations showing the effectiveness of the proposed FRLP and FRGCA modules compared to other design choices for zero-shot performance on DFEW [22].

6. Ethics and Limitations

Ethics Statement. As our approach involves face analysis, we acknowledge ethical concerns related to privacy, bias, and potential misuse. *FaceInstruct-1M* is constructed from publicly available datasets with appropriate licensing, and we release only annotations and instructions, ensuring compliance with data protection regulations like GDPR. However, we recognize that facial recognition technologies may impact privacy and encourage responsible use. Since our dataset is derived from existing sources, it may inherit biases, and addressing these remains for future work. Our research is intended for ethical academic use, and we

strongly discourage any application that infringes on individual rights or promotes discrimination.

Limitations. Face-LLaVA is limited to single-turn interactions and lacks advanced chain-of-thought reasoning. Moreover, we did not explore face identification or dense prediction tasks. Future work can address these limitations by integrating multi-turn dialogue capabilities and expanding to other facial tasks.

7. Conclusions

This work advances MLLMs for facial analysis across diverse tasks, including expression recognition, AU detection, attribute detection, age estimation, and deepfake detection. We introduce *FaceInstruct-1M*, a large-scale dataset with over one million samples, automatically annotated using Gemini and GPT-4o, and propose Face-LLaVA, an MLLM leveraging novel FRLP and FRGCA modules to enrich visual representations for advanced face analysis. Extensive evaluations demonstrate its superiority over open-source MLLMs and competitive performance against task-specific methods, with GPT-4 confirming its advanced reasoning capabilities.

8. Acknowledgements

Research was sponsored by the Army Research Office and was accomplished under Cooperative Agreement Number W911NF-25-2-0040. The views and conclusions contained in this document are those of the authors and should not be interpreted as representing the official policies, either expressed or implied, of the Army Research Office or the U.S. Government. The U.S. Government is authorized to reproduce and distribute reprints for Government purposes notwithstanding any copyright notation herein.

References

- [1] Darius Afchar, Vincent Nozick, Junichi Yamagishi, and Isao Echizen. Mesonet: a compact facial video forgery detection network. In *2018 IEEE International Workshop on Information Forensics and Security (WIFS)*, pages 1–7, 2018. [2](#), [7](#)
- [2] Raphael Angulu, Jules R Tapamo, and Aderemi O Adewumi. Age estimation via face images: a survey. *EURASIP J. Image Video Process.*, 2018(1), 2018. [1](#), [2](#)
- [3] Valentin Bazarevsky, Yury Kartynnik, Andrey Vakunov, Karthik Raveendran, and Matthias Grundmann. Blaze-face: Sub-millisecond neural face detection on mobile gpus. *CoRR*, abs/1907.05047, 2019. [4](#)
- [4] Axel Berg, Magnus Oskarsson, and Mark O’Connor. Deep ordinal regression with label diversity. In *2020 25th International Conference on Pattern Recognition (ICPR)*, pages 2740–2747. IEEE, 2021. [7](#)
- [5] Adrian Bulat and Georgios Tzimiropoulos. How far are we from solving the 2d & 3d face alignment problem? (and a dataset of 230,000 3d facial landmarks). In *International Conference on Computer Vision*, 2017. [6](#), [5](#)
- [6] Zhixi Cai, Shreya Ghosh, Kalin Stefanov, Abhinav Dhall, Jianfei Cai, Hamid Rezaatofghi, Reza Haffari, and Munawar Hayat. Marlin: Masked autoencoder for facial video representation learning. In *Proceedings of the IEEE/CVF Conference on Computer Vision and Pattern Recognition (CVPR)*, pages 1493–1504, 2023. [1](#), [2](#), [7](#)
- [7] Yin Chen, Jia Li, Shiguang Shan, Meng Wang, and Richang Hong. From static to dynamic: Adapting landmark-aware image models for facial expression recognition in videos. *IEEE Transactions on Affective Computing*, pages 1–15, 2024. [1](#), [2](#), [7](#), [16](#)
- [8] Zebang Cheng, Zhi-Qi Cheng, Jun-Yan He, Kai Wang, Yuxiang Lin, Zheng Lian, Xiaojiang Peng, and Alexander G Hauptmann. Emotion-LLaMA: Multimodal emotion recognition and reasoning with instruction tuning. In *The Thirty-eighth Annual Conference on Neural Information Processing Systems*, 2024. [1](#), [2](#), [3](#), [7](#), [4](#), [5](#)
- [9] Francois Chollet. Xception: Deep Learning with Depthwise Separable Convolutions . In *2017 IEEE Conference on Computer Vision and Pattern Recognition (CVPR)*, pages 1800–1807, Los Alamitos, CA, USA, 2017. IEEE Computer Society. [2](#), [7](#)
- [10] Zongyong Deng, Hao Liu, Yaoxing Wang, Chenyang Wang, Zekuan Yu, and Xuehong Sun. Pml: Progressive margin loss for long-tailed age classification. In *2021 IEEE/CVF Conference on Computer Vision and Pattern Recognition (CVPR)*, pages 10498–10507, 2021. [7](#)
- [11] Mohammad Ennab and Hamid Mcheick. Designing an interpretability-based model to explain the artificial intelligence algorithms in healthcare. *Diagnostics (Basel)*, 12(7): 1557, 2022. [1](#)
- [12] Niki M Foteinopoulou, Enjie Ghorbel, and Djamilia Aouada. A hitchhiker’s guide to fine-grained face forgery detection using common sense reasoning. In *Advances in Neural Information Processing Systems*, pages 2943–2976, 2024. [1](#), [3](#)
- [13] Bin-Bin Gao, Hong-Yu Zhou, Jianxin Wu, and Xin Geng. Age estimation using expectation of label distribution learning. In *Proceedings of the 27th International Joint Conference on Artificial Intelligence*, page 712–718. AAAI Press, 2018. [2](#)
- [14] Bin-Bin Gao, Xin-Xin Liu, Hong-Yu Zhou, Jianxin Wu, and Xin Geng. Learning expectation of label distribution for facial age and attractiveness estimation, 2021. [7](#)
- [15] Xuri Ge, Junchen Fu, Fuhai Chen, Shan An, Nicu Sebe, and Joemon M Jose. Towards end-to-end explainable facial action unit recognition via vision-language joint learning. In *Proceedings of the 32nd ACM International Conference on Multimedia*, pages 8189–8198, New York, NY, USA, 2024. ACM. [1](#), [3](#), [7](#)
- [16] Kaiming He, Xinlei Chen, Saining Xie, Yanghao Li, Piotr Dollár, and Ross Girshick. Masked autoencoders are scalable vision learners, 2021. [2](#)
- [17] Edward J Hu, yelong shen, Phillip Wallis, Zeyuan Allen-Zhu, Yuanzhi Li, Shean Wang, Lu Wang, and Weizhu Chen.

- LoRA: Low-rank adaptation of large language models. In *International Conference on Learning Representations*, 2022. 6
- [18] Guohong Hu, Xing Lan, Hanyu Jiang, Jiayi Lyu, and Jian Xue. Towards unified facial action unit recognition framework by large language models, 2024. 3, 7
- [19] Siyuan Hu, Zheng Wang, Peng Hu, Xi Peng, Jie Wu, Hongyuan Zhu, and Yew Soon Ong. Preface: Face-centric pretraining with self-structure aware distillation. *Proceedings of the AAAI Conference on Artificial Intelligence*, 38: 12538–12546, 2024. 2
- [20] Maryam Imani and Gholam Ali Montazer. A survey of emotion recognition methods with emphasis on e-learning environments. *Journal of Network and Computer Applications*, 147:102423, 2019. 1
- [21] Geethu Miriam Jacob and Bjorn Stenger. Facial action unit detection with transformers. In *Proceedings of the IEEE/CVF Conference on Computer Vision and Pattern Recognition*, pages 7680–7689, 2021. 7, 3
- [22] Xingxun Jiang, Yuan Zong, Wenming Zheng, Chuangao Tang, Wanchuang Xia, Cheng Lu, and Jiateng Liu. Dfew: A large-scale database for recognizing dynamic facial expressions in the wild. In *Proceedings of the 28th ACM International Conference on Multimedia*, pages 2881–2889, 2020. 3, 4, 5, 6, 7, 8, 1, 2, 10, 11, 16, 22
- [23] Tero Karras, Samuli Laine, and Timo Aila. A Style-Based Generator Architecture for Generative Adversarial Networks. *IEEE Transactions on Pattern Analysis & Machine Intelligence*, 43(12):4217–4228, 2021. 8
- [24] Michael K Keutmann, Samantha L Moore, Adam Savitt, and Ruben C Gur. Generating an item pool for translational social cognition research: methodology and initial validation. *Behav. Res. Methods*, 47(1):228–234, 2015. 4, 6, 7, 8, 2, 3, 5, 10, 16
- [25] Hasam Khalid, Shahroz Tariq, Minha Kim, and Simon S. Woo. FakeAVCeleb: A novel audio-video multimodal deepfake dataset. In *Thirty-fifth Conference on Neural Information Processing Systems Datasets and Benchmarks Track (Round 2)*, 2021. 3, 4, 5
- [26] Dimitrios Kollias and Stefanos Zafeiriou. Aff-wild2: Extending the aff-wild database for affect recognition, 2019. 3
- [27] Yuanyuan Lei and Houwei Cao. Audio-visual emotion recognition with preference learning based on intended and multi-modal perceived labels. *IEEE Transactions on Affective Computing*, 14(4):2954–2969, 2023. 7, 2
- [28] Bo Li, Yuanhan Zhang, Dong Guo, Renrui Zhang, Feng Li, Hao Zhang, Kaichen Zhang, Yanwei Li, Ziwei Liu, and Chunyuan Li. Llava-onevision: Easy visual task transfer. *arXiv preprint arXiv:2408.03326*, 2024. 1, 7, 8, 2, 3, 4
- [29] Hanting Li, Hongjing Niu, Zhaoqing Zhu, and Feng Zhao. Intensity-aware loss for dynamic facial expression recognition in the wild. *Proc. Conf. AAAI Artif. Intell.*, 37(1):67–75, 2023. 7, 2
- [30] Min Li, Xiaoqin Zhang, Tangfei Liao, Sheng Lin, and Guobao Xiao. Pth-net: Dynamic facial expression recognition without face detection and alignment. *IEEE Transactions on Image Processing*, 34:30–43, 2025. 7, 2, 16, 17
- [31] Shan Li, Weihong Deng, and JunPing Du. Reliable crowdsourcing and deep locality-preserving learning for expression recognition in the wild. In *2017 IEEE Conference on Computer Vision and Pattern Recognition (CVPR)*, pages 2584–2593. IEEE, 2017. 3, 4, 6, 7, 2, 5, 17
- [32] Xiaotian Li, Xiang Zhang, Taoyue Wang, and Lijun Yin. Knowledge-spreader: Learning semi-supervised facial action dynamics by consistifying knowledge granularity. In *2023 IEEE/CVF International Conference on Computer Vision (ICCV)*, pages 20922–20932, 2023. 7, 3
- [33] Yifan Li, Hu Han, Shiguang Shan, zhihong ji, Jinfeng Bai, and Xilin Chen. Recot: Regularized co-training for facial action unit recognition with noisy labels. In *34th British Machine Vision Conference 2023, BMVC 2023, Aberdeen, UK, November 20-24, 2023*. BMVA, 2023. 2, 7, 3
- [34] Yifan Li, Anh Dao, Wentao Bao, Zhen Tan, Tianlong Chen, Huan Liu, and Yu Kong. Facial affective behavior analysis with instruction tuning. *European Conference on Computer Vision (ECCV) 2024*, 2024. 1, 2, 3, 4, 5, 6, 7, 8, 16, 17
- [35] Zheng Lian, Haiyang Sun, Licai Sun, Kang Chen, Mngyu Xu, Kexin Wang, Ke Xu, Yu He, Ying Li, Jinming Zhao, Ye Liu, Bin Liu, Jiangyan Yi, Meng Wang, Erik Cambria, Guoying Zhao, Björn W Schuller, and Jianhua Tao. MER 2023: Multi-label learning, modality robustness, and semi-supervised learning. In *Proceedings of the 31st ACM International Conference on Multimedia*, pages 9610–9614, New York, NY, USA, 2023. ACM. 10
- [36] Zheng Lian, Licai Sun, Mingyu Xu, Haiyang Sun, Ke Xu, Zhuofan Wen, Shun Chen, Bin Liu, and Jianhua Tao. Explainable multimodal emotion reasoning. *arXiv preprint arXiv:2306.15401*, 2023. 2, 3, 6
- [37] Bin Lin, Yang Ye, Bin Zhu, Jiayi Cui, Munan Ning, Peng Jin, and Li Yuan. Video-LLaVA: Learning united visual representation by alignment before projection. In *Proceedings of the 2024 Conference on Empirical Methods in Natural Language Processing*, pages 5971–5984, Miami, Florida, USA, 2024. Association for Computational Linguistics. 3, 5, 6, 7, 8, 2, 4, 17
- [38] Chin-Yew Lin. ROUGE: A package for automatic evaluation of summaries. In *Text Summarization Branches Out*, pages 74–81, Barcelona, Spain, 2004. Association for Computational Linguistics. 4
- [39] Haotian Liu, Chunyuan Li, Qingyang Wu, and Yong Jae Lee. Visual instruction tuning. In *Thirty-seventh Conference on Neural Information Processing Systems*, 2023. 1, 3, 5
- [40] Yuanyuan Liu, Wei Dai, Chuanxu Feng, Wenbin Wang, Guanghao Yin, Jiabei Zeng, and Shiguang Shan. MAFW: A Large-scale, Multi-modal, Compound Affective Database for Dynamic Facial Expression Recognition in the Wild. ACM, New York, NY, USA, 2022. 3, 4, 8, 2, 5, 10
- [41] Yuanyuan Liu, Wenbin Wang, Yibing Zhan, Shaoze Feng, Kejun Liu, and Zhe Chen. Pose-disentangled contrastive learning for self-supervised facial representation. In *Proceedings of the IEEE/CVF Conference on Computer Vision and Pattern Recognition (CVPR)*, pages 9717–9728, 2023. 2
- [42] Ziwei Liu, Ping Luo, Xiaogang Wang, and Xiaoou Tang. Deep learning face attributes in the wild. In *2015 IEEE In-*

- ternational Conference on Computer Vision (ICCV), pages 3730–3738, 2015. 1, 2, 3, 4, 5, 6, 7, 8, 17, 20, 24
- [43] Cheng Luo, Siyang Song, Weicheng Xie, Linlin Shen, and Hatice Gunes. Learning multi-dimensional edge feature-based au relation graph for facial action unit recognition. In *Proceedings of the Thirty-First International Joint Conference on Artificial Intelligence, IJCAI-22*, pages 1239–1246, 2022. 2, 7, 3
- [44] Jiawei Mao, Rui Xu, Xuesong Yin, Yuanqi Chang, Binling Nie, and Aibin Huang. Poster++: A simpler and stronger facial expression recognition network, 2023. 7, 2
- [45] Longbiao Mao, Yan Yan, Jing-Hao Xue, and Hanzi Wang. Deep Multi-Task Multi-Label CNN for Effective Facial Attribute Classification. *IEEE Transactions on Affective Computing*, 13(02):818–828, 2022. 1, 2, 7
- [46] S. Mohammad Mavadati, Mohammad H. Mahoor, Kevin Bartlett, Philip Trinh, and Jeffrey F. Cohn. Disfa: A spontaneous facial action intensity database. *IEEE Transactions on Affective Computing*, 4(2):151–160, 2013. 3, 4, 5, 6, 7, 2, 11, 17, 24
- [47] Ali Mollahosseini, Behzad Hasani, and Mohammad H Mahoor. AffectNet: A database for facial expression, valence, and arousal computing in the wild. *IEEE Trans. Affect. Comput.*, 10(1):18–31, 2019. 3, 4, 7, 5
- [48] Kartik Narayan, Vibashan VS, Rama Chellappa, and Vishal M Patel. Facexformer: A unified transformer for facial analysis. *arXiv preprint arXiv:2403.12960*, 2024. 2
- [49] Kishore Papineni, Salim Roukos, Todd Ward, and Wei-Jing Zhu. Bleu: a method for automatic evaluation of machine translation. In *Proceedings of the 40th Annual Meeting of the Association for Computational Linguistics*, pages 311–318, Philadelphia, Pennsylvania, USA, 2002. Association for Computational Linguistics. 4
- [50] Gan Pei, Jiangning Zhang, Menghan Hu, Zhenyu Zhang, Chengjie Wang, Yunsheng Wu, Guangtao Zhai, Jian Yang, Chunhua Shen, and Dacheng Tao. Deepfake generation and detection: A benchmark and survey, 2024. 1
- [51] Tonya S Pixton. Happy to see me, aren’t you, sally? signal detection analysis of emotion detection in briefly presented male and female faces. *Scand. J. Psychol.*, 52(4):361–368, 2011. 1
- [52] Yuyang Qian, Guojun Yin, Lu Sheng, Zixuan Chen, and Jing Shao. Thinking in frequency: Face forgery detection by mining frequency-aware clues. In *Computer Vision – ECCV 2020*, pages 86–103, Cham, 2020. Springer International Publishing. 2, 7, 8
- [53] Lixiong Qin, Mei Wang, Chao Deng, Ke Wang, Xi Chen, Jiani Hu, and Weihong Deng. Swinface: A multi-task transformer for face recognition, expression recognition, age estimation and attribute estimation. *IEEE Transactions on Circuits and Systems for Video Technology*, 34(4):2223–2234, 2024. 2, 7
- [54] Lixiong Qin, Mei Wang, Xuannan Liu, Yuhang Zhang, Wei Deng, Xiaoshuai Song, Weiran Xu, and Weihong Deng. Facepor: A generalist model for face perception. In *Computer Vision – ECCV 2024*, pages 240–260, Cham, 2025. Springer Nature Switzerland. 1, 2, 7
- [55] Alec Radford, Jong Wook Kim, Chris Hallacy, Aditya Ramesh, Gabriel Goh, Sandhini Agarwal, Girish Sastry, Amanda Askell, Pamela Mishkin, Jack Clark, Gretchen Krueger, and Ilya Sutskever. Learning transferable visual models from natural language supervision, 2021. 2
- [56] K. Ricanek and T. Tesafaye. Morph: a longitudinal image database of normal adult age-progression. In *7th International Conference on Automatic Face and Gesture Recognition (FG06)*, pages 341–345, 2006. 3, 4, 6, 7, 5, 11, 17
- [57] Andreas Rössler, Davide Cozzolino, Luisa Verdoliva, Christian Riess, Justus Thies, and Matthias Nießner. FaceForensics++: Learning to detect manipulated facial images. In *International Conference on Computer Vision (ICCV)*, 2019. 3, 4, 5, 6, 7, 8, 11, 17, 21, 23
- [58] Ethan M. Rudd, Manuel Günther, and Terrance E. Boulton. Moon: A mixed objective optimization network for the recognition of facial attributes. In *Computer Vision – ECCV 2016*, pages 19–35, Cham, 2016. Springer International Publishing. 2, 7
- [59] Zhiwen Shao, Zhilei Liu, Jianfei Cai, and Lizhuang Ma. Jânnet: Joint facial action unit detection and face alignment via adaptive attention. *International Journal of Computer Vision*, 129:321 – 340, 2020. 2, 7, 3
- [60] Yichun Shi, Xiang Yu, Kihyuk Sohn, Manmohan Chandraker, and Anil K. Jain. Towards universal representation learning for deep face recognition. In *Proceedings of the IEEE/CVF Conference on Computer Vision and Pattern Recognition (CVPR)*, 2020. 2
- [61] Yan Shi, Zijun Zhang, Kaining Huang, Wudi Ma, and Shanshan Tu. Human-computer interaction based on face feature localization. *Journal of Visual Communication and Image Representation*, 70:102740, 2020. 1
- [62] Nyeong-Ho Shin, Seon-Ho Lee, and Chang-Su Kim. Moving window regression: A novel approach to ordinal regression. In *2022 IEEE/CVF Conference on Computer Vision and Pattern Recognition (CVPR)*, pages 18739–18748, 2022. 2, 7
- [63] Haomiao Sun, Mingjie He, Tianheng Lian, Hu Han, and Shiguang Shan. Face-mllm: A large face perception model, 2024. 3
- [64] Licai Sun, Zheng Lian, Bin Liu, and Jianhua Tao. Mae-dfer: Efficient masked autoencoder for self-supervised dynamic facial expression recognition. In *Proceedings of the 31st ACM International Conference on Multimedia*, page 6110–6121, 2023. 2, 7
- [65] Yang Tang, Wangding Zeng, Dafei Zhao, and Honggang Zhang. Piap-df: Pixel-interested and anti person-specific facial action unit detection net with discrete feedback learning. In *2021 IEEE/CVF International Conference on Computer Vision (ICCV)*, pages 12879–12888, 2021. 2, 7, 3
- [66] Gemini Team. Gemini 1.5: Unlocking multimodal understanding across millions of tokens of context, 2024. 4, 7, 2, 3, 5
- [67] OpenAI Team. Gpt-4o mini: advancing cost-efficient intelligence. <https://openai.com/index/gpt-4o-mini-advancing-cost-efficient-intelligence/>, 2024. [Accessed 25-02-2025]. 2, 4, 6, 7, 3, 17

- [68] Qwen Team. Qwen2.5-vl, 2025. 3, 7, 8, 2, 4, 18
- [69] Zhan Tong, Yibing Song, Jue Wang, and Limin Wang. VideoMAE: Masked autoencoders are data-efficient learners for self-supervised video pre-training. In *Advances in Neural Information Processing Systems*, 2022. 2
- [70] Hanyang Wang, Bo Li, Shuang Wu, Siyuan Shen, Feng Liu, Shouhong Ding, and Aimin Zhou. Rethinking the learning paradigm for dynamic facial expression recognition. In *2023 IEEE/CVF Conference on Computer Vision and Pattern Recognition (CVPR)*, pages 17958–17968, 2023. 2, 7, 16
- [71] Junke Wang, Zuxuan Wu, Wenhao Ouyang, Xintong Han, Jingjing Chen, Yu-Gang Jiang, and Ser-Nam Li. M2TR: Multi-modal multi-scale transformers for deepfake detection. In *Proceedings of the 2022 International Conference on Multimedia Retrieval*, New York, NY, USA, 2022. ACM. 7
- [72] Yan Wang, Yixuan Sun, Yiwen Huang, Zhongying Liu, Shuyong Gao, Wei Zhang, Weifeng Ge, and Wenqiang Zhang. Ferv39k: A large-scale multi-scene dataset for facial expression recognition in videos. In *Proceedings of the IEEE/CVF Conference on Computer Vision and Pattern Recognition*, pages 20922–20931, 2022. 3, 4, 2, 5, 10
- [73] Yan Wang, Shaoqi Yan, Yang Liu, Wei Song, Jing Liu, Yang Chang, Xinji Mai, Xiping Hu, Wenqiang Zhang, and Zhongxue Gan. A survey on facial expression recognition of static and dynamic emotions, 2024. 1
- [74] Chongke Wu, Sicong Shao, Cihan Tunc, Pratik Satam, and Salim Hariri. An explainable and efficient deep learning framework for video anomaly detection. *Cluster Comput.*, 25(4):2715–2737, 2022. 1
- [75] Peihao Xiang, Kaida Wu, Chaohao Lin, and Ou Bai. Mtcaedf: Multi-task cascaded autoencoder for dynamic facial expression recognition, 2024. 2, 7, 16, 17
- [76] Hongxia Xie, Chu-Jun Peng, Yu-Wen Tseng, Hung-Jen Chen, Chan-Feng Hsu, Hong-Han Shuai, and Wen-Huang Cheng. Emovit: Revolutionizing emotion insights with visual instruction tuning. In *Proceedings of the IEEE/CVF Conference on Computer Vision and Pattern Recognition (CVPR)*, 2024. 1, 3
- [77] Bohao Xing, Zitong Yu, Xin Liu, Kaishen Yuan, Qilang Ye, Weicheng Xie, Huanjing Yue, Jingyu Yang, and Heikki Kälviäinen. Emo-llama: Enhancing facial emotion understanding with instruction tuning, 2024. 3, 7, 2
- [78] Xiaogang Xu, Hengshuang Zhao, Vibhav Vineet, Ser-Nam Lim, and Antonio Torralba. Mtformer: Multi-task learning via transformer and cross-task reasoning. In *Computer Vision – ECCV 2022*, pages 304–321, Cham, 2022. Springer Nature Switzerland. 7, 2
- [79] Fanglei Xue, Qiangchang Wang, and Guodong Guo. TransFER: Learning Relation-aware Facial Expression Representations with Transformers. In *2021 IEEE/CVF International Conference on Computer Vision (ICCV)*, pages 3581–3590, Los Alamitos, CA, USA, 2021. IEEE Computer Society. 1, 2, 7, 17
- [80] Fanglei Xue, Qiangchang Wang, Zichang Tan, Zhongsong Ma, and Guodong Guo. Vision transformer with attentive pooling for robust facial expression recognition. *IEEE Transactions on Affective Computing*, 14(4):3244–3256, 2023. 2, 7, 17
- [81] Boqiang Zhang, Kehan Li, Zesen Cheng, Zhiqiang Hu, Yuqian Yuan, Guanzheng Chen, Sicong Leng, Yuming Jiang, Hang Zhang, Xin Li, et al. Videollama 3: Frontier multi-modal foundation models for image and video understanding. *arXiv preprint arXiv:2501.13106*, 2025. 3, 7, 8, 1, 2, 4, 18, 21
- [82] Tengan Zhang, Chuanhe Liu, Xiaolong Liu, Yuchen Liu, Liyu Meng, Lei Sun, Wenqiang Jiang, Fengyuan Zhang, Jinming Zhao, and Qin Jin. Multi-task learning framework for emotion recognition in-the-wild. In *Computer Vision – ECCV 2022 Workshops*, pages 143–156, Cham, 2023. Springer Nature Switzerland. 7, 2
- [83] Xing Zhang, Lijun Yin, Jeffrey F. Cohn, Shaun Canavan, Michael Reale, Andy Horowitz, Peng Liu, and Jeffrey M. Girard. Bp4d-spontaneous: a high-resolution spontaneous 3d dynamic facial expression database. *Image and Vision Computing*, 32(10):692–706, 2014. Best of Automatic Face and Gesture Recognition 2013. 3, 4, 6, 7, 2, 5, 11, 17
- [84] Yuhang Zhang, Chengrui Wang, and Weihong Deng. Relative uncertainty learning for facial expression recognition. In *Advances in Neural Information Processing Systems*, pages 17616–17627. Curran Associates, Inc., 2021. 2, 7
- [85] Yuhang Zhang, Chengrui Wang, Xu Ling, and Weihong Deng. Learn from all: Erasing attention consistency for noisy label facial expression recognition. In *Computer Vision – ECCV 2022*, pages 418–434, Cham, 2022. Springer Nature Switzerland. 2, 7
- [86] Yuanhan Zhang, Jinming Wu, Wei Li, Bo Li, Zejun Ma, Ziwei Liu, and Chunyuan Li. Video instruction tuning with synthetic data, 2024. 1, 3, 7, 2, 18
- [87] Zhifei Zhang, Yang Song, and Hairong Qi. Age progression/regression by conditional adversarial autoencoder. In *IEEE Conference on Computer Vision and Pattern Recognition (CVPR)*. IEEE, 2017. 3, 4, 5, 6, 7, 17, 25
- [88] Fufangchen Zhao, Ming Li, Linrui Xu, Wenhao Jiang, Jian Gao, and Danfeng Yan. Favchat: Unlocking fine-grained facial video understanding with multimodal large language models, 2025. 3
- [89] Zengqun Zhao and Qingshan Liu. Former-dfer: Dynamic facial expression recognition transformer. In *Proceedings of the 29th ACM International Conference on Multimedia*, pages 1553–1561, 2021. 7, 2
- [90] Yinglin Zheng, Hao Yang, Ting Zhang, Jianmin Bao, Dongdong Chen, Yangyu Huang, Lu Yuan, Dong Chen, Ming Zeng, and Fang Wen. General facial representation learning in a visual-linguistic manner. In *Proceedings of the IEEE/CVF Conference on Computer Vision and Pattern Recognition*, pages 18697–18709, 2022. 3
- [91] Yinglin Zheng, Hao Yang, Ting Zhang, Jianmin Bao, Dongdong Chen, Yangyu Huang, Lu Yuan, Dong Chen, Ming Zeng, and Fang Wen. General facial representation learning in a visual-linguistic manner. In *Proceedings of the IEEE/CVF conference on computer vision and pattern recognition*, pages 18697–18709, 2022. 2

- [92] Ruicong Zhi, Mengyi Liu, and Dezheng Zhang. A comprehensive survey on automatic facial action unit analysis. *Vis. Comput.*, 36(5):1067–1093, 2020. [1](#)
- [93] Bin Zhu, Bin Lin, Munan Ning, Yang Yan, Jiaxi Cui, WANG HongFa, Yatian Pang, Wenhao Jiang, Junwu Zhang, Zongwei Li, Cai Wan Zhang, Zhifeng Li, Wei Liu, and Li Yuan. Languagebind: Extending video-language pretraining to n-modality by language-based semantic alignment. In *The Twelfth International Conference on Learning Representations*, 2024. [2](#), [5](#)
- [94] Hao Zhu, Wayne Wu, Wentao Zhu, Liming Jiang, Siwei Tang, Li Zhang, Ziwei Liu, and Chen Change Loy. CelebV-HQ: A large-scale video facial attributes dataset. In *ECCV*, 2022. [1](#), [3](#)

Face-LLaVA: Facial Expression and Attribute Understanding through Instruction Tuning

Supplementary Material

Table of Contents

• Ethics Statement	Appendix A
• Limitations and Future Work	Appendix B
• Detailed Results	Appendix C
• Task-specific Datasets Used	Appendix D
• Additional Details about FaceInstruct-1M	Appendix E
• Evaluation	Appendix F
• Implementation Details	Appendix G
• Reasoning Comparison with Baselines	Appendix H
• Failure Cases	Appendix I

A. Ethics Statement

As the proposed approach involves face analysis, we acknowledge the ethical considerations associated with privacy, bias and potential misuse.

Privacy and data protection. *FaceInstruct-1M* is constructed using existing task-specific datasets with appropriate licensing for research use. We will only release the annotations and instructions for *FaceInstruct-1M* and not the video or images from the individual data sources, and the users of the dataset are recommended to obtain the videos from their original sources with appropriate consent. We do not collect or use private user data, ensuring compliance with data protection regulations such as GDPR. However, we recognize that facial recognition technologies may pose risks to individual privacy, and we encourage responsible use of our dataset and model.

Bias and fairness. Facial analysis models often exhibit biases due to imbalanced training data, leading to disparities in performance across different demographic groups. Since our dataset is based on existing datasets for face analysis, it inherits some biases that are already present in those datasets. Evaluation of model bias is however left as a future work.

Responsible use. Face analysis technologies have applications in various domains, including healthcare and accessibility. However, they also present risks if misused for mass surveillance, or profiling. Our research is intended for academic and ethical use, and we strongly discourage any application that infringes upon individuals’ rights, promotes discrimination, or compromises security.

We believe in transparency and open research. Upon acceptance, we will release our dataset and model to support further advancements in social AI development.

B. Limitations and Future Work

While this work demonstrates pioneering efforts in using MLLMs for general face analysis, there are some limitations that can be addressed by future works. First, Face-LLaVA is trained on single-turn conversations and hence lacks advanced abilities such as conversationing and chain-of-thought reasoning. Such training will require augmenting *FaceInstruct-1M* with conversation and reasoning data. Second, we only explored face-perception tasks and not face recognition or dense prediction tasks. While reasoning makes less sense in some of those tasks, there exists a potential to explore the performance of MLLMs on other facial tasks. Finally, since our dataset is automatically annotated using closed-source MLLMs, Gemini and GPT4, it contains some noise introduced by model hallucinations.

C. Detailed Results

This section contains detailed results from Sec. 5.

Facial expression recognition. Tab. 7 is an expanded version of Tab. 3 and contains the individual class recall values for the DFEW [22] dataset. We can observe that Face-LLaVA achieves better recall than the baselines on classes that are underrepresented in the data (disgust and fear). We noticed that some of the MLLM baselines are biased towards some expression categories, which is also evident by their recall values. For example, VideoLLaMA 3 [81] is biased towards the disgust and fear classes, while performing poorly on classes that other models are good at.

DFEW [22]										Crema-D [24]			RAF-DB [31]	
Method	Hap ↑	Sad ↑	Neu ↑	Ang ↑	Sur ↑	Dis ↑	Fea ↑	UAR ↑	WAR ↑	Method	UAR ↑	WAR ↑	Method	Acc. ↑
<i>Closed - source models</i>														
GPT4o-mini [67]	0.847	0.859	0.221	0.392	0.331	0.048	0.284	0.426	0.518	GPT4o-mini [67]	0.410	0.486	GPT4o-mini [67]	0.758
Gemini-1.5F [66]	0.646	0.762	0.357	0.287	0.320	0.227	0.435	0.433	0.481	Gemini-1.5F [66]	0.465	0.635	Gemini-1.5F [66]	0.685
<i>Zero-shot</i>														
Vid.LLaMA 3 [81]	0.619	0.131	0.502	0.031	0.000	0.364	0.357	0.286	0.305	Vid.LLaMA 3 [81]	0.397	0.546	Vid.LLaMA 3 [81]	0.671
Qwen 2.5 [68]	0.199	0.424	0.945	0.072	0.310	0.000	0.100	0.293	0.399	Qwen 2.5 [68]	0.395	0.566	Qwen 2.5 [68]	0.526
Vid.-LLaVA [37]	0.663	0.000	0.772	0.009	0.006	0.091	0.0	0.220	0.326	Vid.-LLaVA [37]	0.367	0.557	Vid.-LLaVA [37]	0.545
LLaVA-Vid. [86]	0.639	0.671	0.807	0.097	0.012	0.000	0.286	0.375	0.498	LLaVA-Vid. [86]	0.478	0.618	LLaVA-OV [28]	0.700
EmoLA [*] [34]	0.548	0.589	0.383	0.587	0.214	0.000	0.106	0.346	0.449	EmoLA [*] [34]	0.431	0.618	EmoLA [34]	0.741
Emotion LLaMA [†] [8]	0.720	0.763	0.620	0.719	0.337	0.000	0.033	0.456	0.594	Emotion LLaMA [8]	0.225	0.308		
Emotion LLaMA [‡] [8]	0.412	0.516	0.289	0.444	0.351	0.000	0.100	0.302	0.378					
Face-LLaVA (Ours)	0.639	0.809	0.582	0.471	0.316	0.136	0.329	0.469	0.564	Face-LLaVA (Ours)	0.582	0.681	Face-LLaVA (Ours)	0.780
<i>Fine-tuned</i>														
EC-STFL [22]	0.792	0.491	0.579	0.610	0.461	0.028	0.215	0.454	0.565	Lei et al. [27]	0.645	0.648	RUL [84]	0.890
Former-DFER [89]	0.841	0.626	0.675	0.700	0.564	0.035	0.318	0.537	0.657	PTH-Net [30]	0.699	0.700	EAC [85]	0.909
GCA-IAL [29]	0.880	0.672	0.701	0.761	0.622	0.000	0.264	0.557	0.692	MAE-DFER [64]	0.773	0.774	TransFER [79]	0.909
M3DFEL [70]	0.896	0.684	0.679	0.742	0.597	0.000	0.316	0.561	0.693	MTL-ER* [82]	0.745	0.756	Xue et al. [80]	0.920
MAE-DFER [64]	0.929	0.775	0.746	0.769	0.610	0.186	0.424	0.634	0.744	MT-Former* [78]	0.793	0.807	POSTERv2 [44]	0.922
S2D [7]	0.936	0.803	0.771	0.811	0.645	0.014	0.347	0.618	0.760	MTCAE-DFER [75]	0.847	0.850	EmoLA [34]	0.921
EMO-LLaMA [77]	-	-	-	-	-	-	-	0.602	0.659					
Emotion-LLaMA [8]	0.931	0.794	0.725	0.841	0.728	0.035	0.442	0.642	0.771					
Face-LLaVA (Ours)	0.873	0.924	0.653	0.798	0.586	0.136	0.401	0.625	0.745	Face-LLaVA (Ours)	0.798	0.813	Face-LLaVA (Ours)	0.921

Table 7. Comparison of the proposed approach with recent MLLMs and supervised techniques for emotion recognition on the DFEW [22], Crema-D [24] and RAF-DB [31] dataset. *:Only using middle video frame, †: Results taken from the paper [8], ‡: Results computed after running inference code on face-cropped video.

Action unit detection. Tabs. 8 and 9 expand Tab. 4 to show the F1 scores for individual action units. Notice that for the finetuning setting on DISFA [46], Face-LLaVA not only outperforms the baselines on average F1 score, but achieves the best F1 score on majority of the possible AUs in the dataset. A similar observation can be made for the analysis on the BP4D dataset [83] in Tab. 9.

GPT Evaluation. We report the mean GPT-4o-mini scores for all the tasks and scoring criterias in Tab. 10. For all five tasks, the reasoning capabilities of Face-LLaVA generated results are rated higher than the baselines. Moreover, the high consistency of reasoning with ground truth suggests that Face-LLaVA provides a description or reason that aligns with the correct ground truth label. Notice that for AU detection, all the general MLLMs perform poorly compared to Face-LLaVA and manual verification of the results revealed that these models have less knowledge about the Facial Action Unit Coding System (FACS) and hence their outputs include hallucinations. To compare the quality of responses generated by our model in comparison to the baselines, please refer to Appendix H.

D. Task-specific datasets used

As mentioned in Sec. 3, *FaceInstruct-1M* is constructed using task-specific face analysis datasets for facial expression recognition, facial action unit detection, age estimation, facial attributes detection and deepfake detection. We present a summary of these datasets in this section. We refer the readers to Appendix F for a detailed description of the evaluation protocol on these datasets.

D.1. Facial Expression Recognition

Dynamic Facial Expression in-the-Wild (DFEW) [22] is a large-scale facial expression dataset comprising 16,372 video clips sourced from movies. Each clip is manually annotated by 12 expert annotators, with 10 independent labels per clip. The dataset includes seven basic emotion categories: happiness, sadness, neutral, anger, surprise, fear, and disgust. Although some clips have multiple emotion labels, we observed that the perceived emotion is often ambiguous in these cases. Therefore, we conduct all experiments on the single-labeled subset of 11.7k clips. As a multimodal dataset, DFEW contains audio and background context (e.g., multiple actors, body gestures), meaning the emotion labels may not be solely based on facial expressions.

MAFW [40] is another large-scale dynamic facial expression dataset containing approximately 10k movie clips. Each clip is annotated by 11 professional annotators for 11 emotion categories, including the seven basic emotions plus contempt, anxiety, helplessness, and disappointment. However, since these additional emotion categories have relatively few samples, we exclude them from our experiments. Like DFEW, MAFW is a multimodal dataset containing audio.

FERV39k [72] is a large-scale multi-scene dataset featuring 39k video samples, each categorized into one of seven basic

Method	AU1 ↑	AU2 ↑	AU4 ↑	AU6 ↑	AU9 ↑	AU12 ↑	AU25 ↑	AU26 ↑	Avg. F1 ↑
<i>Closed-source models</i>									
GPT-4o-mini [66]	0.292	0.302	0.565	0.416	0.493	0.244	0.582	0.536	0.429
Gemini-1.5F [66]	0.504	0.558	0.421	0.376	0.512	0.405	0.724	0.624	0.515
<i>Zero-shot</i>									
VideoLLaMA 3 [81]	0.101	0.253	0.394	0.369	0.450	0.395	0.493	0.534	0.374
Qwen 2.5 VL [68]	0.204	0.291	0.664	0.571	0.468	0.301	0.478	0.475	0.431
Video-LLaVA [37]	0.167	0.368	0.459	0.518	0.508	0.532	0.501	0.483	0.442
LLaVA-OV [28]	0.044	0.143	0.201	0.146	0.469	0.182	0.520	0.535	0.280
EmoLA [34]	0.193	0.141	0.406	0.513	0.434	0.515	0.608	0.535	0.418
Face-LLaVA (Ours)	0.517	0.650	0.551	0.578	0.530	0.511	0.571	0.521	0.553
<i>Fine-tuned</i>									
ATCM [21]	0.461	0.486	0.728	0.567	0.500	0.721	0.908	0.554	0.615
ReCoT [33]	0.513	0.362	0.668	0.501	0.524	0.788	0.953	0.697	0.626
KS [32]	0.538	0.599	0.692	0.542	0.508	0.758	0.922	0.468	0.628
ME-GraphAU [43]	0.546	0.471	0.729	0.540	0.557	0.767	0.911	0.530	0.631
JAA-Net [59]	0.624	0.607	0.671	0.411	0.451	0.735	0.909	0.674	0.635
PIAP-DF [65]	0.502	0.518	0.719	0.506	0.545	0.797	0.941	0.572	0.638
VL-FAU [15]	0.609	0.564	0.740	0.463	0.608	0.724	0.943	0.665	0.665
AU-LLaVA [18]	0.520	0.592	0.444	0.308	0.223	0.661	0.908	0.546	0.525
EmoLA [34]	0.505	0.569	0.835	0.552	0.431	0.801	0.916	0.600	0.651
Face-LLaVA (Ours)	0.636	0.623	0.790	0.733	0.710	0.832	0.902	0.606	0.729

Table 8. Comparison of the proposed approach with recent MLLMs and supervised techniques on the 8 AUs of the DISFA [46] dataset.

Method	AU1 ↑	AU2 ↑	AU4 ↑	AU6 ↑	AU7 ↑	AU10 ↑	AU12 ↑	AU14 ↑	AU15 ↑	AU17 ↑	AU23 ↑	AU24 ↑	Avg. F1 ↑
<i>Closed-source models</i>													
GPT4o-mini [67]	0.458	0.449	0.630	0.618	0.331	0.393	0.660	0.525	0.516	0.440	0.465	0.462	0.496
Gemini-1.5F [66]	0.533	0.556	0.606	0.687	0.487	0.432	0.756	0.395	0.543	0.427	0.466	0.493	0.532
<i>Zero-shot</i>													
VideoLLaMA 3 [81]	0.426	0.450	0.444	0.488	0.448	0.362	0.508	0.417	0.502	0.454	0.499	0.498	0.458
Qwen 2.5 VL [68]	0.260	0.422	0.549	0.702	0.328	0.503	0.579	0.441	0.455	0.446	0.459	0.461	0.467
VideoLLaVA [37]	0.477	0.495	0.461	0.396	0.296	0.470	0.357	0.491	0.489	0.459	0.470	0.483	0.445
LLaVA-OV [28]	0.342	0.427	0.373	0.473	0.392	0.335	0.454	0.482	0.462	0.505	0.516	0.507	0.439
EmoLA [34]	0.185	0.143	0.584	0.541	0.304	0.266	0.647	0.375	0.419	0.500	0.450	0.468	0.407
Face-LLaVA (Ours)	0.494	0.498	0.648	0.687	0.312	0.295	0.746	0.375	0.510	0.445	0.462	0.470	0.495
<i>Fine-tuned</i>													
JAA-Net [59]	0.538	0.478	0.582	0.785	0.758	0.827	0.882	0.637	0.433	0.618	0.456	0.499	0.624
PIAP-DF [65]	0.542	0.471	0.540	0.790	0.782	0.863	0.895	0.661	0.497	0.632	0.499	0.520	0.641
ATCM [21]	0.517	0.493	0.610	0.778	0.795	0.829	0.863	0.676	0.519	0.630	0.437	0.563	0.642
ReCoT [33]	0.515	0.478	0.589	0.792	0.802	0.849	0.884	0.616	0.533	0.646	0.518	0.554	0.648
ME-GraphAU (SWIN) [43]	0.527	0.443	0.609	0.799	0.801	0.853	0.892	0.694	0.554	0.644	0.498	0.551	0.655
AU-LLaVA [18]	0.582	0.459	0.619	0.786	0.756	0.878	0.905	0.590	0.324	0.625	0.305	0.403	0.603
EmoLA [34]	0.574	0.524	0.610	0.781	0.778	0.819	0.895	0.605	0.493	0.649	0.460	0.524	0.642
VL-FAU [15]	0.563	0.499	0.626	0.795	0.801	0.826	0.886	0.668	0.513	0.635	0.513	0.571	0.658
Face-LLaVA (Ours)	0.541	0.610	0.642	0.801	0.663	0.718	0.861	0.644	0.566	0.627	0.579	0.649	0.658

Table 9. Comparison of the proposed approach with recent MLLMs and supervised techniques on the 12 AUs of the BP4D [83] dataset.

emotions across 22 different scene types. The dataset is annotated through crowd-sourcing and professional annotators, with 30 independent annotations per clip. Unlike DFEW and MAFW, FERV39k does not contain audio, but it still includes background information such as multiple actors, body movements, and hand gestures, which can influence perceived emotions.

Crema-D [24] is a emotional multimodal dataset, containing 7,442 clips from 91 actors, including 48 male and 43 females. They are between 20 and 74, from a variety of races and ethnicities. The actors spoke 12 sentences, which were presented using one of 6 emotion categories, and four different emotion levels. The dataset is annotated by 2,443 participants, promising 95% of the clips have more than 7 ratings.

AffectNet [47] is a large-scale facial expression dataset containing more than 1M facial images. The dataset is collected by querying 1250 emotion related keywords in 6 different languages on the Internet with three major search engines. About half

Method	Reason-Video Consistency						Reason-GT Consistency						Reasoning Completeness					
	Emo.	AU	Attr.	Age	DF.	All	Emo.	AU	Attr.	Age	DF.	All	Emo.	AU	Attr.	Age	DF.	All
GT from <i>FaceInstruct-1M</i>	9.47	8.52	9.80	9.27	8.85	9.18	9.70	8.84	9.88	9.55	9.56	9.51	9.21	8.26	9.75	9.02	8.41	8.93
VideoLLaMA 3 [81]	5.14	2.58	6.90	5.82	7.02	5.49	5.27	2.06	6.27	5.13	7.64	5.27	4.90	2.73	6.50	5.37	6.51	5.20
Qwen 2.5 VL [68]	5.82	3.02	5.48	7.36	5.48	5.43	5.96	2.54	4.86	7.02	5.76	5.23	5.57	3.34	5.21	6.89	5.30	5.26
Video LLaVA [37]	4.31	2.58	5.82	7.79	6.19	5.34	4.47	2.06	5.28	7.10	6.58	5.10	4.20	2.73	5.30	7.00	5.84	5.01
LLaVA-OV [28]	7.11	2.18	6.08	7.97	6.69	6.01	7.30	1.95	5.48	7.44	7.33	5.9	6.67	2.34	5.72	7.52	6.19	5.69
EmoLA [34]	7.33	5.17	-	-	-	-	7.58	5.04	-	-	-	-	6.81	5.32	-	-	-	-
Emotion-LLaMA [8]	6.77	-	-	-	-	-	6.90	-	-	-	-	-	6.50	-	-	-	-	-
Face-LLaVA (Ours)	7.95	6.90	8.34	7.68	8.56	7.89	8.14	6.68	8.13	7.53	9.20	7.94	7.79	6.62	7.89	7.59	8.11	7.60

Table 10. Mean GPT4o ratings (on a scale of 1-10) for different methods in a zero-shot setting on the *FaceInstruct-1M* Test Set.

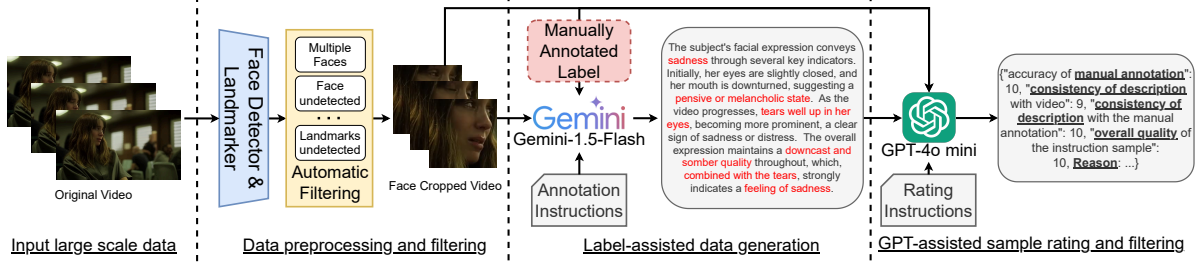


Figure 5. Data annotation pipeline used for creating *FaceInstruct-1M* dataset.

of the retrieved images were manually annotated with seven facial expression categories.

RAF-DB [31] is a large-scale facial expression dataset, containing 29,672 facial images with a variety of age, gender and ethnicity. It is annotated by 40 independent annotators. EM algorithm was applied to filter out unreliable labels.

D.2. Action Unit Detection

DISFA [46] is a non-posed facial expression dataset containing videos of 27 adults with different ethnicities, with high resolution. All video frames are annotated by two human FACS experts for the intensity of AUs (0-5 scale).

BP4D [83] is a 3D video database of facial expressions of 41 young adults between ages 18 to 29, The dataset is manually annotated with 12 action units, and contains automatically tracked head pose and 2D/3D facial landmarks.

D.3. Facial Attribute Detection

CelebA [42] is a large-scale face attributes dataset, containing more than 200K celebrity images, each with 40 attribute annotations. CelebA includes images with large diversity in pose and background.

D.4. Age Estimation

MORPH II [56] is a dataset containing 55134 mugshots, annotated with age estimate, gender, and race classification.

UTKFace [87] is a large-scale face dataset with people aged between 0 to 116 years old, containing over 20K images annotated with age, gender, and ethnicity.

D.5. Deepfake Detection

FaceForensics++ [57] is a dataset consisting of 1000 original video sequence, manipulated with 4 face manipulation methods: Deepfakes, Face2Face, FaceSwap, and NeuralTextures. The videos were generated from 977 YouTube source videos.

Fake AV-Celeb [25] is a dataset that includes about 20K manipulated videos generated using various deepfake synthesis methods. The base set consists of 500 real videos of celebrities from YouTube.

E. Additional details about FaceInstruct-1M

Fig. 5 illustrates the annotation pipeline used to create our dataset from a large-scale, manually annotated dataset.

E.1. Data preprocessing

As mentioned in Sec. 3.1 and shown in Fig. 5, we pre-process the visual inputs, i.e. images and videos in each of the constituent datasets before getting the annotations from Gemini. We use Mediapipe [3] with default parameters to detect face

Dataset	Task	Number of Samples		
		Initial	After Preproc.	After GF.
DFEW [22]	Expression	11.7k	6.7k	6.2k
MAFW [40]	Expression	10k	6.9k	6.6k
FERV39k [72]	Expression	39k	30.7k	28.8k
Crema-D [24]	Expression	7.4k	7.4k	6.8k
AffectNet [47]	Expression	287k	280k	260k
RAF-DB [31]	Expression	15k	15k	14.8k
DISFA [46]	AU	131k	130k	123k
BP4D [83]	AU	150k	146k	128k
CelebA [42]	Attributes	203k	201k	196k
UTK Face [87]	Age	24.1k	23.5k	22.8k
MORPH II [56]	Age	50k	49.9k	49k
FaceForensics++ [57]	Deepfake	30k	25.9k	24.7k
Fake AV-Celeb [25]	Deepfake	20k	19.5k	19.3k
Real Faces* [22, 40, 72]	Deepfake	60.7k	44.3k	43.8k
Total	-	1.04M	987k	930k

Table 11. Statistics about data preprocessing and GPT-filtering (GF.) of for each of the constituent datasets of *FaceInstruct-1M*. *: Real faces augmentation for deepfake detection task is created from DFEW, MAFW and FERV39k.

bounding boxes within the video or image. For video datasets, we filter away all the videos in which the face of the subject goes out of the frame and cases where multiple faces are detected. We do not apply any smoothing to the detection bounding boxes for videos as we found that such smoothing fails in cases where the subject’s face has a sudden movement and hence, in such cases, the face moves out of the smoothed bounding box. We do not align the faces after cropping because for some tasks such as facial expression recognition, certain head movements such as nodding and head shakes might contain signals to predict and reason the correct output. After cropping the face bounding box from a video or an image, we resize the image into 256x256 for all downstream processing and training.

After face cropping, we used FAN [5] for detecting 68 2-D facial landmarks for all the samples in constituent datasets. We filter away all the samples in which landmark is not detected even in one of the frames of the video. Such, strict filtering ensures high data quality.

We report the statistics of our data after preprocessing in Tab. 11. Note that for FaceForensics++ [57] dataset, since the number of samples in the training set are quite small (only 4k), we split the dataset into chunks of 3 seconds and use those for all the processing.

E.2. Getting descriptions/reasoning from Gemini

We use Gemini-1.5 Flash [66] for getting all the data annotations for constituent datasets. Note that Gemini-2.0 was still under an experimental phase during the creation of *FaceInstruct-1M* so we used Gemini-1.5 Flash. Fig. 6 illustrates the prompts that we have used to get annotations from Gemini. Note that we do some prompt tuning for each task and provide negative prompts to control the output format, and to restrict the model from generating disclaimers. Moreover, we explicitly prompt the model to not mention that it has been provided with the ground truth information so that the generated descriptions can directly be used for prompt tuning.

It is also important to note that for the deepfake detection and age estimation tasks, we explicitly ask the model to start its response with the ground truth label so that it is easier to parse the responses, when computing traditional metrics for these datasets.

E.3. Task-specific instructions

To train our model on *FaceInstruct-1M* dataset, we need task-specific instructions for different tasks. To that extent, we carefully collected 100 handcrafted instructions for each of the five tasks. Some example instructions for different tasks are illustrated in Fig. 7. Notice that since the instructions for a particular task are semantically similar, we can use the instructions randomly during training similar to [8] during training. Note that we replace the ‘video’/‘image’ string in the instruction with appropriate type of data depending on the current sample.

The given video has {cur_emotion} emotion. Your task is to reason why the emotion is tagged as "{cur_emotion}". Focus specifically on the facial expression of the subject in the video and describe how it varies.

Give your response in JSON format as following {"emotion":"angry","reason":"reason for your response"}. Strictly follow this format and add details in the reason field of the JSON.

In your provided reason, do not mention that I gave you any prior information about the video.

Facial Expression Recognition

This image is taken from a Facial Action Unit Detection Dataset. According to the dataset, {cur_AU_list} is/are activated in the given image. Please describe why you think {cur_AU_list} is/are activated.

Give your response in JSON format as following {"AU":["AU1", "AU2"],"reason":"reason for your response"}. The field "AU" within the json is a list containing the AUs that are activated on this image depending on your answer. Strictly follow this format and add details in the reason field of the JSON.

In your provided reason, do not mention that I gave you any prior information about the image.

Action Unit Detection

This image is marked to have the following attributes - {cur_attr_list}. Write a paragraph with a few sentences describing the facial attributes of this image. Make sure to use the exact same string attributes as given before in your description. DO NOT Modify the strings in the attributes for each attribute.

Give your response in JSON format as following {"reason":"string describing the facial attributes of the image and reason for any"}. Strictly follow this format and if an attribute is not obvious, then try to reason why that attribute is linked to the image.

In your provided reason, do not mention that I gave you any prior information about the image.

Facial Attribute Detection

The person in this image is {cur_age} years old. Reason why you think the person is {cur_age} years old based on the facial features, hair or anything else.

Give your response in JSON format as following {"age":"10","reason":"reason for your response"}. The field "reason" should start with the age of the person and then following the reason for your answer. Strictly follow this format and add details in the reason field of the JSON.

In your provided reason, do not mention that I gave you any prior information about the image.

Age Estimation

This video has been [manipulated by a deepfake technique](#). Describe the details of the face and video as well that does not seem real in this video as compared to a real video. Please DO NOT describe anything else in the video and avoid any disclaimers.

Give your response in JSON format as following {"fake":"yes","reason":"reason for your response"}. The field "fake" within the json can take values "yes" or "no" depending on whether the given video is fake or not. Start your reason with the word "Real" or "Fake" depending on the case. Strictly follow this format and add details in the reason field of the JSON.

In your provided reason, do not mention that I gave you any prior information about the video.

Deepfake Detection (for fake videos)

This video is [downloaded from youtube](#). Describe the details of face and video as well that make this a real and non-manipulated video. Please DO NOT describe anything else in the video and avoid any disclaimers.

Give your response in JSON format as following {"fake":"yes","reason":"reason for your response"}. The field "fake" within the json can take values "yes" or "no" depending on whether the given video is fake or not. Start your reason with the word "Real" or "Fake" depending on the case. Strictly follow this format and add details in the reason field of the JSON.

In your provided reason, do not mention that I gave you any prior information about the video.

Deepfake Detection (for real videos)

Figure 6. Prompts used for generating descriptions or reasoning from Gemini-1.5 Flash. Notice that we pass the label information about the data through [blue text](#).

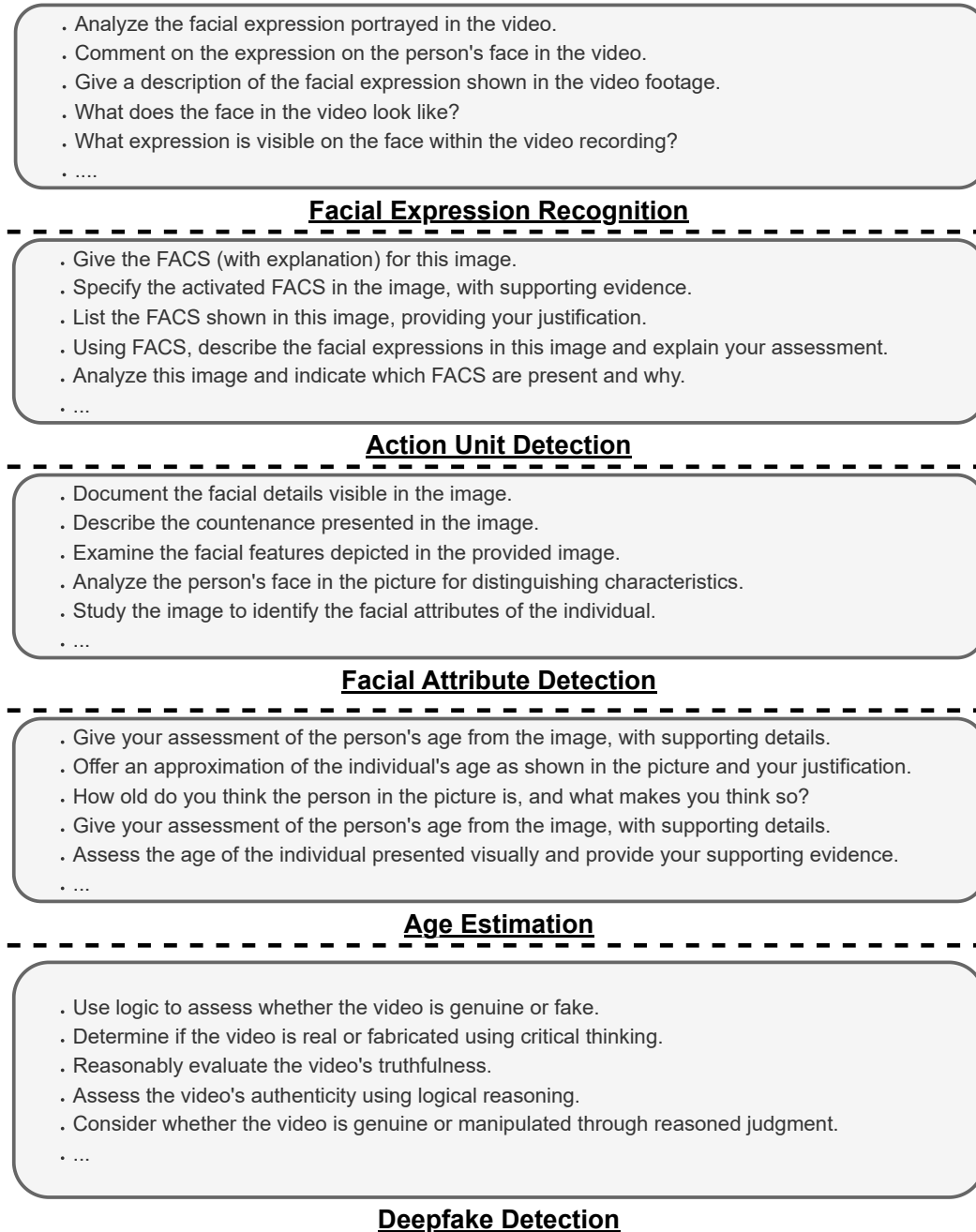


Figure 7. Samples of various instructions used for different face analysis tasks. Note that for each task, the instructions are analogous which allows us to use them randomly with any sample belonging to that task during training, thereby augmenting the data size.

E.4. GPT-4 Filtering

As mentioned in Sec. 3.2, we employ GPT4o-mini to rate the annotations obtained from Gemini to perform additional filtering. Moreover, this automated rating works as a sanity check to understand the quality of annotations generated from Gemini. Fig. 8 shows the rating instructions or prompts that we use for GPT4 assisted rating. We rate the annotations for all the prompts on the same four criteria - (i) accuracy of the manually annotated label w.r.t. the face-cropped video, (ii) consistency of the generated description with the face-cropped video, (iii) consistency of the generated description with the manually annotated label, and (iv) overall quality of the sample based on resolution, visibility of the face, etc. Moreover, we

also ask the model to provide a short reason for its ratings to assist us in determining the reason for an unexpectedly high or low rating. Tab. 11 summarizes the number of videos that are filtered after GPT filtering. As mentioned in Sec. 3.2, we filter away all the samples with an overall rating less than or equal to 6, thereby resulting in about 7% of the initial dataset getting filtered away.

You are given 8 frames uniformly sampled from a video along with a description for the facial expression with reason for the video. You are also provided with the ground truth categorical emotional label associated with the video.

Your task is to rate the given video and description pair on a scale of 1(lowest) to 10(highest) based on the following metrics -

- (1) Accuracy of the given ground truth categorical label with respect to the video.
- (2) Consistency of the given description with respect to the video.
- (3) Consistency of the given description with respect to the ground truth label.
- (4) Overall quality of this video-description pair.

Your output should be in JSON format as following {"rating":{"1":"rating for task 1", "2"...}, "reason":"short reason for ratings if any"}.

"Categorical Label": "{**cur_emotion**}"

"Description": "{**desc**}"

Facial Expression Recognition

You are given an image along with a description for the facial action units activated with reason for the image. You are also provided with the ground truth action units (FACS-coded) associated with the image.

Your task is to rate the given image and description pair on a scale of 1(lowest) to 10(highest) based on the following metrics -

- (1) Accuracy of the given ground truth action unit labels with respect to the image.
- (2) Consistency of the given description with respect to the image.
- (3) Consistency of the given description with respect to the ground truth label.
- (4) Overall quality of this image-description pair.

Your output should be in JSON format as following {"rating":{"1":"rating for task 1", "2"...}, "reason":"short reason for ratings if any"}.

"Action Unit Label": "{**cur_AU_list**}"

"Description": "{**desc**}"

Action Unit Detection

You are given an image along with a description for the face attributes present in the image with reason associated with them. You are also provided with the ground truth face-attributes associated with the image.

Your task is to rate the given image and description pair on a scale of 1(lowest) to 10(highest) based on the following metrics -

- (1) Accuracy of the given ground truth face attribute labels with respect to the image.
- (2) Consistency of the given description with respect to the image.
- (3) Consistency of the given description with respect to the ground truth label.
- (4) Overall quality of this image-description pair.

Your output should be in JSON format as following {"rating":{"1":"rating for task 1", "2"...}, "reason":"short reason for ratings if any"}.

"Face Attributes Label": "{**cur_attr_list**}"

"Description": "{**desc**}"

Facial Attribute Detection

You are given an image along with a description for the estimated age of the person in the image with reason associated with them. You are also provided with the ground truth age associated with the person in the image.

Your task is to rate the given image and description pair on a scale of 1(lowest) to 10(highest) based on the following metrics -

- (1) Accuracy of the given ground truth age with respect to the image.
- (2) Consistency of the given description with respect to the image.
- (3) Consistency of the given description with respect to the ground truth age.
- (4) Overall quality of this image-description pair.

Your output should be in JSON format as following {"rating":{"1":"rating for task 1", "2"...}, "reason":"short reason for ratings if any"}.

"Ground Truth Age": "{**cur_age**}"

"Description": "{**desc**}"

Age Estimation

You are given 8 frames uniformly sampled from a video along with a description for the authenticity or forgery for the video. You are also provided with the ground truth associated with the video.

Your task is to rate the given video and description pair on a scale of 1(lowest) to 10(highest) based on the following metrics -

- (1) Accuracy of the given ground truth categorical label with respect to the video.
- (2) Consistency of the given description with respect to the video.
- (3) Consistency of the given description with respect to the ground truth label.
- (4) Overall quality of this video-description pair.

Your output should be in JSON format as following {"rating":{"1":"rating for task 1", "2"...}, "reason":"short reason for ratings if any"}.

"Categorical label": "{**real/fake**}"

"Description": "{**desc**}"

Deepfake Detection

Figure 8. Rating instructions (Prompts) used for data filtering using GPT4o-mini. Notice that we pass the label information about the data and the description generated from Gemini through **blue text**.

Constituents	Labels used	GPT-filtering	No. of samples	DFEW [22]	
				UAR	WAR
M, F, C	✗	✗	44.7k	0.298	0.350
M, F, C, MER	✗	✗	89.7k	0.293	0.355
M, F, C	✗	✓	15.4k	0.318	0.375
M, F, C, MER	✗	✓	25.9k	0.327	0.392
M, F, C	✓	✗	44.7k	0.415	0.501
M, F, C	✓	✓	40.2k	0.424	0.520

Table 12. Ablations showing the effectiveness of using annotation labels for data generation and GPT filtering on zero-shot model performance on DFEW [22] dataset. M:MAFW [40], D: DFEW [22], F:FERV39k [72], C: Crema-D [24], MER: MER2023 [35].

E.5. Ablation for data annotation pipeline

To demonstrate the effectiveness of incorporating labels as additional signals and applying GPT-4o-mini filtering during dataset construction, we conduct ablation experiments on a subset of *FaceInstruct-1M* for zero-shot expression recognition on DFEW [22]. As baseline datasets for this study, we use MAFW [40], FERV39k [72], and Crema-D [24]. Additionally, to assess whether increasing the number of unlabeled samples improves performance, we include an unlabeled dataset from MER2023 [35], containing approximately 45k samples.

Tab. 12 summarizes our findings. The results indicate a significant performance improvement when leveraging ground truth labels from constituent datasets to generate annotations using Gemini. Unlike traditional self-supervised learning approaches, where increasing data volume typically enhances performance, we observe that adding more unlabeled data does not lead to better task performance – an important consideration for face analysis. Finally, filtering the dataset with GPT-4o-mini results in additional performance gain, as the data is labeled by one expert model (Gemini) and subsequently rated and filtered by another (GPT), improving overall data quality.

(a) Facial Expression Recog.

(b) Action Unit Detection

(c) Facial Attribute Detection

(d) Deepfake Detection

(e) Age Estimation

Video durations. Fig. 9 shows the distribution of video durations for video-related tasks in *FaceInstruct-1M*. The total duration of videos for facial expression recognition is around 35 hours, with a mean of 2.28 seconds, and that of deepfake detection is around 84 hours, with a mean of 3.87 seconds. We can observe that the median duration is around 2 seconds for facial expression recognition while it is around 3-4 seconds for deepfake detection. It is also important to mention that since the FaceForensics++ [57] dataset has longer videos, we chunk the videos into smaller ones of around 3 seconds.

Word Clouds. Fig. 10 shows the word clouds generated for the descriptions or reasons for the samples belonging to different tasks present in *FaceInstruct-1M*. Word cloud for facial expression recognition further highlights the bias in the dataset for *happiness* class with the word cloud for *happiness* and *smile* being big. Similarly, the word cloud for facial attribute detection correlates with the class distribution for facial attribute detection. It is important to note that all of the word clouds have bigger clouds for face or face regions (such as mouth, eyes, lip, nose, hair) important for reasoning on that task. For example, for deepfake detection, since the texture of skin plays an important role, so *skin* has a larger cloud.

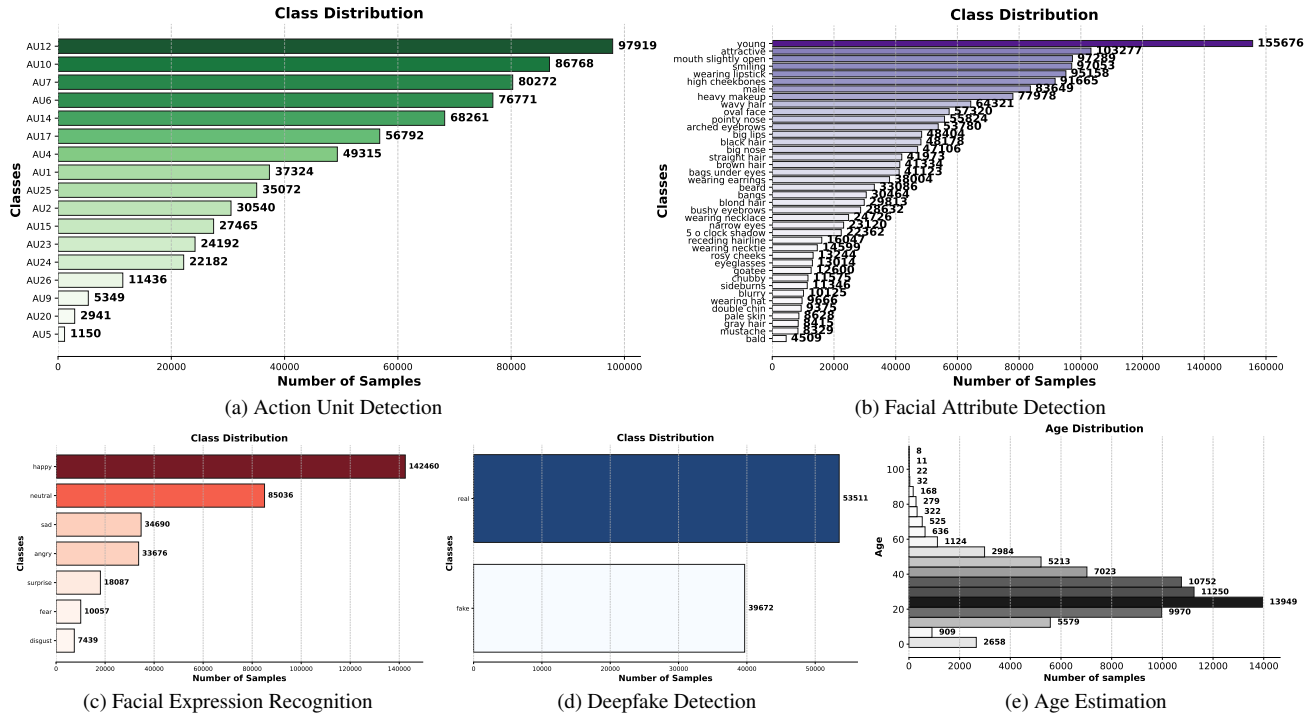


Figure 11. Class distribution for different face tasks present in *FaceInstruct-1M*.

E.7. Data samples

Figs. 12 to 16 show samples of reasoning or descriptions for different tasks present in *FaceInstruct-1M*. Notice in Fig. 12 that the annotations not only capture the overall emotion of the video, but they also contain information about how the facial expression and facial movements varied throughout the video to reason the overall emotion. For facial expression recognition, it is also important to note that in addition to the 7 emotion categories, the annotations also capture sub-emotions or feelings such as revulsion, distaste, etc.

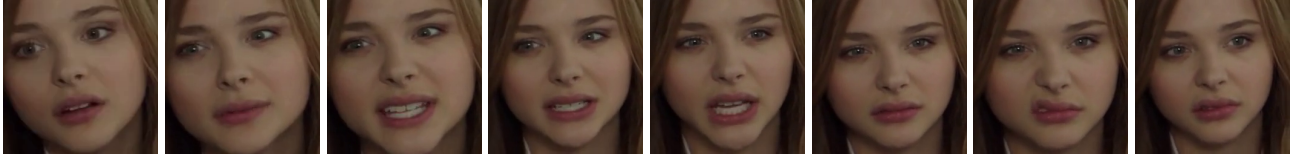
For deepfake detection (Fig. 13), the annotations successfully capture the necessary imperfections or alterations that are visible in the video frames. Moreover, we can also observe that such descriptions incorporate references to different face regions which highlights the importance of different face regions for different face tasks.

For action unit detection (Fig. 14), the annotations capture the overall facial expression in addition to the action units or facial muscle movements responsible for the facial expressions. Thus, such annotations not only contain information about action units activated in the image, but also provide pseudo data for facial expression recognition. This shows how annotations for one task may help improving performance in a related task.

In Fig. 15, we can see that the annotations for facial attribute detection are pretty short and straightforward as they capture features or attributes that are clearly visible in the image without the need to "reason" a particular aspect of the image. Fig. 16 shows the annotations for age estimation task. For this task, notice that since we have prompted Gemini to start descriptions with the ground truth age (see Fig. 6), so all the descriptions start with the ground truth age. This is done to ease string parsing as mentioned later in Appendix F.2.



The baby's facial expression is the primary indicator of happiness. Initially, a small, gentle smile is present, with the corners of the mouth slightly turned upwards. The eyes are wide and bright, adding to the overall impression of contentment. As the video progresses, the baby's mouth opens and closes, appearing as if babbling happily, and the smile remains consistent though it varies in intensity, sometimes becoming a wider, more pronounced smile. There are no furrowed brows or other features associated with negative emotions. The overall expression consistently conveys a sense of joy and positivity.



The subject's facial expression starts with a neutral look, then transitions to a slight grimace, particularly noticeable around the mouth and nose. Her lips are slightly pursed, and the corners of her mouth are turned down. The eyebrows remain relatively unchanged, however, there is a slight wrinkling around the nose which is a common indicator of disgust. The overall expression conveys a sense of revulsion or distaste, leading to the classification of the emotion as disgust.



The subject's facial expression initially shows a neutral or slightly apprehensive look. Her eyes are wide but not excessively so, and her mouth is slightly open in a way that doesn't immediately suggest shock or fear. However, as the video progresses, the widening of her eyes becomes more pronounced, indicating a sudden and unexpected realization. This intensification of the eye widening, coupled with the slight parting of her lips, is a classic indicator of surprise. It's a shift from a relatively calm expression to one clearly showing astonishment or unexpectedness. The change in her expression is rapid and significant, highlighting the sudden nature of the surprise.

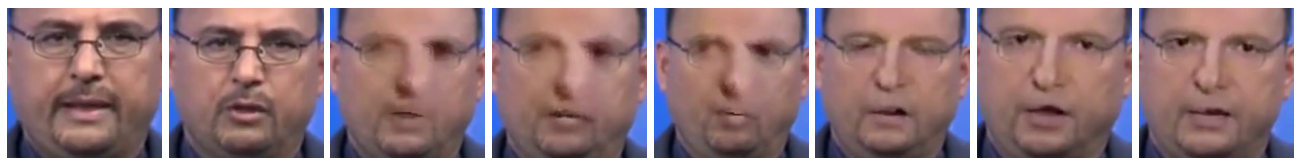
Figure 12. Examples of facial expression recognition task from *FaceInstruct-1M*.



Fake: The face in the video exhibits unnatural transitions and inconsistencies in lighting and shading, particularly around the nose and mouth area, which is typical of face-swapping techniques. There's a lack of natural blending between the swapped face and the original video's background, which makes the face appear pasted onto the video rather than naturally integrated. The subtle micro-expressions and natural movements of the eyes and mouth seem inconsistent with the rest of the face, also a common indicator of face-swapping. The overall texture and color of the skin don't fully match the background, adding to the artificial look.



Fake video. Real skin texture and movement are not consistent. The face shows unnatural blurring and smoothing, particularly around the eyes and mouth, indicating artificial manipulation. The subtle movements of the face lack the natural nuances of real facial expressions; transitions between expressions seem jerky and unrealistic. There is a lack of fine detail in the skin; for example, pores and blemishes are missing, which would be expected in a real video.



Fake: The face in the video is clearly manipulated. Real skin texture and movement are inconsistent throughout the clip. The face appears to shift and distort unnaturally, particularly around the eyes and nose, indicating a poor quality face swap. The lighting and shadowing on the face also don't match the background consistently. These inconsistencies are hallmarks of a Faceswap technique gone wrong.

Figure 13. Examples of deepfake detection task from *FaceInstruct-1M*.

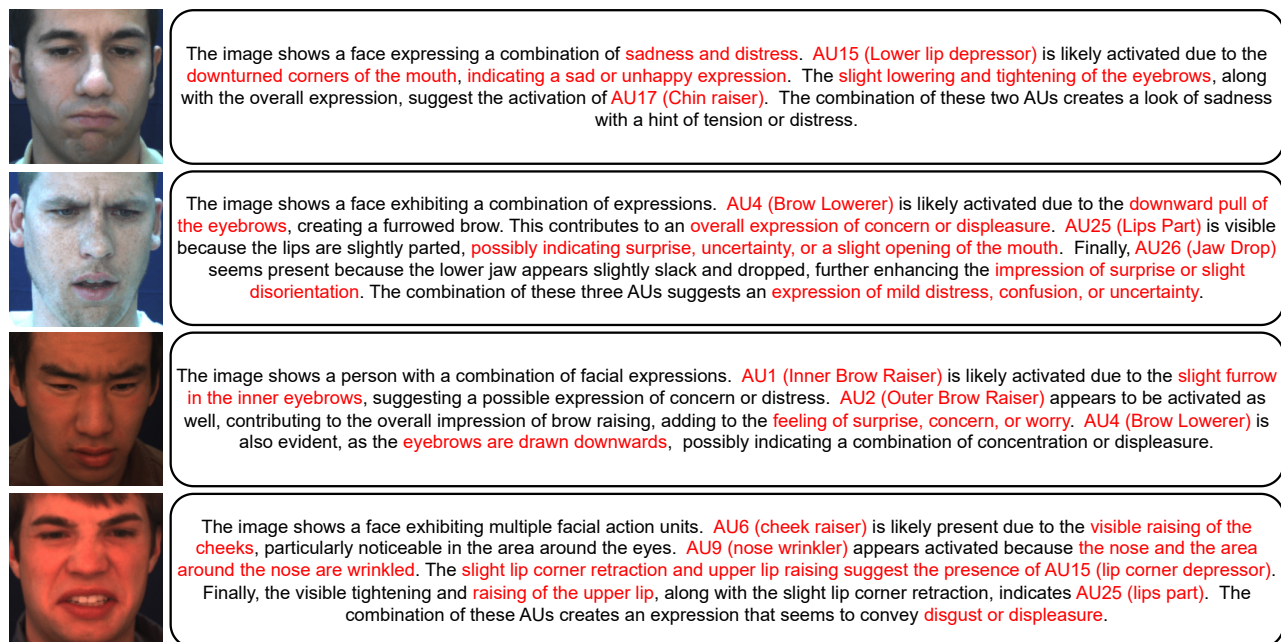


Figure 14. Examples of action unit detection task from *FaceInstruct-1M*.

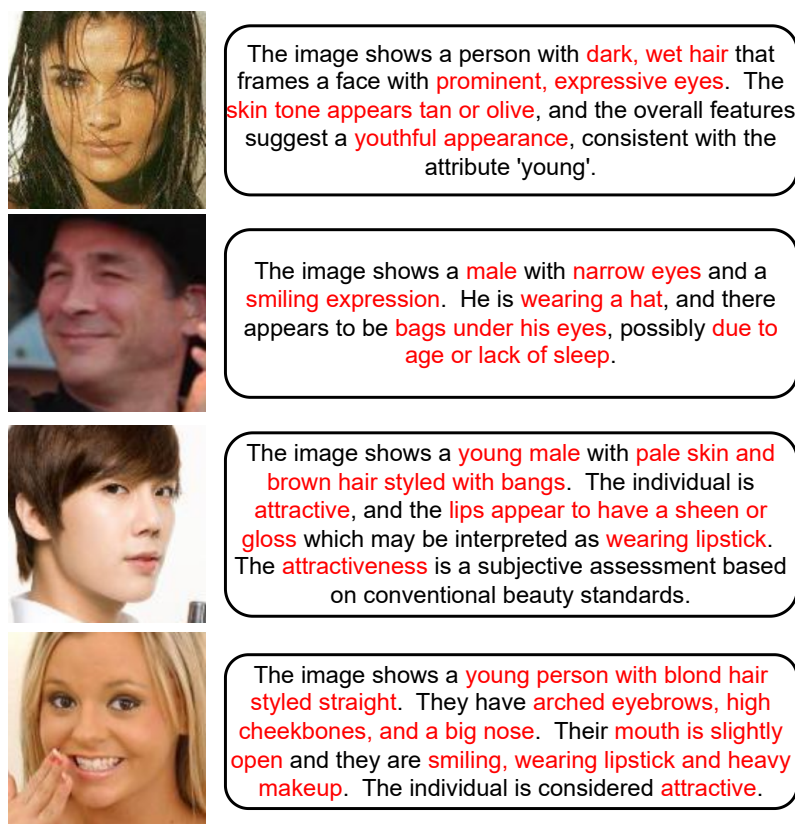


Figure 15. Examples of facial attribute detection task from *FaceInstruct-1M*.



22 years old is a reasonable estimation based on several facial features. The person exhibits a **relatively smooth complexion with minimal visible wrinkles or lines**, suggesting a younger age. The overall shape of the face and the **lack of significant bone structure changes** points towards someone in their early twenties. Additionally, the **person's hairstyle and makeup style** are consistent with those typically associated with young adults in this age range. It's important to note that this is an estimation based on visual cues and could be inaccurate.



85 years old is a reasonable estimate based on the **extensive wrinkling and age spots visible on the skin**. The **deep creases around the eyes, mouth, and forehead** suggest a long history of facial muscle movement and sun exposure. **The thinning of the hair** and the overall texture of the skin also align with the aging process typically seen in someone of this age. While it is difficult to assign a precise age from a photograph, the combination of these features strongly points towards an advanced age within the 80-85 year range.



45 years old is an estimation based on several observable facial features. The individual exhibits **moderate to significant skin texture and some visible lines around the eyes and mouth**, suggesting a person in their **mid-40s**. The **hairline appears to be slightly receding**, which is a common occurrence at this age. The overall facial structure and features show **signs of aging** consistent with a person of this age range. It's important to note that this is an estimation based on visual cues, and individual aging varies greatly.



1 year old: The baby's facial features are consistent with a child of this age. The baby has a **relatively smooth complexion with minimal wrinkles or lines**. The **cheeks are full and round**, which is typical for infants under the age of two. **The size and shape of the head** are also indicative of a baby around one year old. The **presence of only a few teeth** is also consistent with a child who is approximately one year old.

Figure 16. Examples of age estimation task from *FaceInstruct-IM*.

Expression Recognition					Attribute Detection					Deep-Fake Detection	
Happiness	Sadness	Neutral	Anger	...	Attractive	Chubby	Rosy Cheeks	Young	...	Real	Fake
cheerful	crying	calm	annoyed		appealing	plump	blushed cheeks	childish		authentic	fabricated
content	distress	expressionless	enraged		beautiful	puffy face	flushed cheeks	juvenile		genuine	forged
joy	melancholy	unemotional	incensed		good looking	soft cheeks	pinkish cheeks	teenager		legitimate	fraudulent
smiling	sob	unmoving	mad		handsome	round face	red cheeks	youthful		original	manipulated
...

Table 13. Synonyms used for categorizing descriptions into labels for different tasks. We have not shown the complete list of synonyms for all the classes to keep the table succinct.

F. Evaluation

F.1. Synonyms matching

As mentioned in Sec. 3.4, to evaluate the performance of the text generation MLLMs such as Face-LLaVA on traditional face analysis benchmarks, we need to convert the generated text into a prediction label. To that extent we follow synonym matching similar to [34] for facial expression recognition, facial attribute detection and deepfake detection, to categorize the given reason or description to one of the classes. We analyzed the top words from the annotated descriptions of different classes across all tasks and compiled a list of mutually exclusive synonyms for each class, as shown in Tab. 13. For each of the classes within the before-mentioned tasks, we come up with a list of at least 10 synonyms to match to based on the top words occurring in descriptions of our dataset.

Similar to FABAIInstruct [34], to map a given description to a class, we first remove all the negative sentences from the description. Then, we first match for synonyms on the first sentence of the description. If there are matches in the first sentence, then we output the majority voted class to be the dominant class in the given description. If the first sentence did not result in any synonym matches, then we perform majority voting on the entire description. The intuition behind matching the first sentence first is that the response from MLLMs starts with a conclusion or summary sentence and later sentences contain detailed description and reasoning over the first sentence.

While synonyms matching works in an expected way for facial expression recognition and facial attribute detection, manual verification of the descriptions revealed that for deepfake detection the model response might sometimes contain synonyms related to the wrong class more than the predicted class. Since we use majority rating, this would result in the response getting classified to the wrong class even if the response predicts the correct predicted class. To overcome this challenge, we explicitly prompt to start the description of the current sample with the ground truth label of the image (see Fig. 6). While this restricts the description quality in terms of variety in responses, it makes automatic string parsing to extract model prediction from the description easier. Moreover, the goal of this work is not to show that the model can generate varied responses, but rather to exhibit the reasoning capabilities of MLLMs for face-related tasks. Hence, training with such annotations makes Face-LLaVA generate responses that are easier to parse automatically.

F.2. String parsing

For the age estimation and deepfake detection tasks, we simply use regex parsing to convert the given description to categorical or numerical labels (after removing the negative sentences from the description). This works quite well for the AU detection task in fetching the FACS codes from the description, however, for age estimation, sometimes the description contains numerical values other than what the model wants to predict (see Fig. 21). Similar to the previous paragraph for deepfake detection, during data annotation through Gemini, we explicitly prompt to start the description of the current sample with the ground truth age of the person (see Fig. 6).

F.3. Traditional metrics and evaluation protocol

Facial Expression Recognition. For DFEW [22] and Crema-D [24] datasets, similar to previous works [7, 30, 70, 75], we report weighted average recall (WAR) and unweighted average recall (UAR), as the class distribution in these datasets are quite imbalanced. WAR captures the model’s ability to perform well on the majority classes of the dataset. It is calculated as the weighted sum of the recall scores for each class and the weights are determined by the number of samples belonging to a class. Unweighted average recall captures model’s ability to perform well on all the classes including the under-represented classes. It is computed as the average of the recall scores for each class. For DFEW [22], we used the official five-fold cross validation splits to report all the numbers and for Crema-D [24] we perform subject-exclusive 5-fold cross validation to report

```
{...Same instructions as Dataset Rating...}

(1) Consistency or overlap of the given description with respect to the video.
(2) Consistency or overlap of the given description with respect to the ground truth label.
(3) Overall completeness of the description to reason the ground truth label with respect to the video.

{...Same output instructions as Dataset Rating...}
```

Figure 17. Instructions for GPT4o-mini automatic evaluation of the reasoning capabilities of different models. Note that we only change the rating criterias from Fig. 8 to the ones mentioned above to obtain GPT-ratings for the given reasoning outputs for different models.

the results consistent with the baselines [30, 75]. For RAF-DB [31] dataset, similar to the previous baselines [34, 79, 80] we report just the overall accuracy on the official test set consisting of about 3k examples.

Action Unit Detection. In line with the previous works we perform subject exclusive cross validation for reporting our results on BP4D [83] and DISFA [46]. For both the datasets, we report the average F1 score over the set of possible AUs. For DISFA, the available AUs are AU1, AU2, AU4, AU6, AU9, AU12, AU25 and AU26, while for BP4D the AU list contains AU1, AU2, AU4, AU6, AU7, AU10, AU12, AU14, AU15, AU23 and AU24.

Facial Attribute Detection. We report the mean accuracy over each of the 40 facial attributes in the test set of CelebA [42] dataset containing around 20k images.

Age Estimation. For both MORPH II [56] and UTKFace [87] datasets, we report the mean absolute error between the ground truth and the predicted integer ages on the official test splits for both the datasets. For MORPH II, the test set consists of around 5k images and for UTKFACE the test set consists around 4k images.

Deepfake Detection. We use the official test split of FaceForensics++ [57] dataset to report our numbers. We only use the low quality samples from the dataset for both constructing the *FaceInstruct-1M* dataset (and training) and testing. For all the zero-shot MLLM baselines, we chunk the test videos into a constant duration of three seconds and compute the prediction of a video as the majority voted prediction over its constituent chunks. Since for the MLLM baselines and Face-LLaVA, we can only get a text output for this task, so we only report the accuracy on the test set. Note that, the test set of FF++ is imbalanced and has 80% fake videos and only 20% real videos, hence making 80% accuracy as a baseline.

F.4. GPT-Evaluation

As mentioned in Sec. 5.1, we employ GPT4o-mini [67] for automatically evaluating the reasoning capabilities of baselines in comparison to Face-LLaVA. The instructions (prompts) used for this evaluation are similar to those described in Fig. 8 for dataset rating and filtering. We only change the criterias for evaluating the descriptions to those described in Fig. 17 for this evaluation.

G. Implementation details

G.1. Face-LLaVA

To implement our model, we start with the baseline architecture of Video-LLaVA [37] which has a Vicuna-7B backbone and add our novel FRLP and FRGCA modules (as described in Sec. 4) on top of it. To keep the extra computation introduced by the projection layers minimal, we use single layer MLPs within FRLP, as opposed to a 2-layer MLP with GeLU used in the vision projector [37]. Moreover, we only use a single block of cross-attention inside FRGCA with 8 attention heads. We do not apply layer normalization to the output of FRGCA. Maximum context window of the LLM is 2048 tokens and maximum context window of the tokenizer is 3072.

For training, we use deepspeed¹ to parallelize training on a single NVIDIA DGX node with 8*H100 GPUs. We train the model using an AdamW optimizer only for one epoch for both the stages. Face-Region Pretraining takes about 5 hours and Finetuning takes around 12 hours on the entire dataset for the abovementioned environment. Learning rates for the pretraining and finetuning stages are kept as 1e-4 and 2e-5 respectively with cosine learning rate schedule.

G.2. Baselines

We use the official inference code of the baselines. For models which can handle both video and images, we use the corresponding inference code for video and image related tasks. To ensure a fair comparison, for models which have an option to

¹<https://www.deepspeed.ai/>

set the fps [68, 81, 86] for extracting frames for video inputs, we set the fps in such a way that we extract either 8 frames or frames at 1 fps, whichever leads to higher number of frames.

Since we do not finetune the baseline MLLMs and simply use their pretrained weights for inference, we engineer our prompts for each task and model pair to ensure optimum results. For fixed-set prediction tasks such as facial expression recognition, facial attribute detection and deepfake detection, we provide the list of possible classes in the prompt to supervise and restrict the model responses. Moreover, for all the tasks we use a separate prompt for reasoning evaluation and evaluation using traditional metrics. This is done because the responses generated by MLLMs are sometimes hard to parse with the techniques mentioned in Appendices F.1 and F.2. So to report the performance of baselines for Sec. 5.2 we explicitly prompt the baselines to generate its response as a single word or a list of words.


H. Reasoning comparison with baselines

In this section, we illustrate the reasoning capabilities of Face-LLaVA in comparison to the baseline MLLMs. For each task, we pick diverse samples from the *FaceInstruct-1M* test set to show the comparison. Figs. 18 to 22 show this comparison in detail. Readers are encouraged to refer to the caption of these figures for a detailed description about the samples.

I. Failure cases

This section contains the failure cases for Face-LLaVA for different tasks. Figs. 23 to 27 show examples for each of the tasks where Face-LLaVA gives slightly inconsistent responses. In most of the cases, the inaccuracy of prediction with the ground truth label is due to a corner case (multiple expressions present in the face, no action unit activated, etc.) or when the prediction is difficult to make even for humans (deepfake detection and age estimation). In almost all the cases the model output and descriptions align with the video or the image thereby showing excellent vision language grounding for facial tasks.

Ground Truth Label: FEAR



Video-LLaMA 3: The person in the video is **making a funny face** with their **mouth open and eyes wide**, showing a **playful and expressive** demeanor.

Qwen 2.5 VL: The facial expression in the video appears to be **Disgust**. The person's **eyes are narrowed**, and their **mouth is open** in a way that suggests they are **expressing disgust or aversion** to something.


Video-LLaVA: The person in the video has a **smiling facial expression**, which indicates that they are **happy or content**. This could be due to various reasons, such as receiving good news, enjoying a pleasant conversation, or simply having a positive outlook on life. The smile is a universal symbol of happiness and can convey a sense of warmth and friendliness.

LLaVA-Video: The facial expression in the video is **Disgust**. The person's **mouth is slightly open**, and their **eyebrows are raised**, which are common indicators of disgust.

Emotion-LLaMA: The facial expression of the character in the picture is a **neutral one**, with a **slightly raised eyebrow and an open mouth**, which suggests that they are not particularly emotional or expressive the character's body language, including their posture and hand positioning, is also neutral, **with their arms at their sides** and no visible tension or movement this combination of facial and body language cues implies that the **character is likely feeling a sense of calmness or indifference**, rather than any strong emotions

Face-LLaVA (Ours): The subject's facial expression **strongly indicates fear**. **Initially**, their **eyes are wide** and slightly narrowed, suggesting a sense of apprehension or alarm. The mouth is slightly open, possibly in a gasp or a silent scream. **As the video progresses**, the **expression intensifies**; the eyes remain wide, and the mouth continues to be slightly open, possibly indicating a **heightened state of fear or panic**. The overall expression is one of **distress and anxiety**, consistent with the emotion of fear.

Ground Truth Label: SADNESS



Video-LLaMA 3: The person in the video has a **sad face**, which is evident from their facial expression. The reason for this sad expression is not explicitly stated in the video, but it could be inferred that the person is experiencing **some form of emotional distress or sadness**.

Qwen 2.5 VL: The facial expression in the video appears to be **neutral**. The person's **mouth is closed**, and there are no visible signs of anger, happiness, sadness, disgust, fear, or surprise. The **eyes are slightly narrowed**, which could **indicate a neutral or contemplative state**.


Video-LLaVA: The person in the video has a **frowning facial expression**, which indicates that they are **unhappy or dissatisfied**. This could be due to various reasons, such as a recent event, a personal issue, or simply a momentary mood. The frown on their face suggests that they are not in a happy or positive state at the moment.

LLaVA-Video: The facial expression in the video is **neutral**. The person's **eyes are closed**, and there is **no visible smile or frown**.

Emotion-LLaMA: The man in the picture has a **sad expression** on his face, which suggests that **he is feeling emotional or upset** his eyebrows are furrowed, and his eyes appear to be **downcast**, indicating a **sense of melancholy** the overall tone of the image is somber, which further supports the idea that the man is experiencing negative emotions

Face-LLaVA (Ours): The subject's facial expression conveys **sadness** through several cues. **Initially**, his eyebrows are slightly furrowed, and his gaze is downcast, suggesting a **pensive or melancholic state**. His mouth is slightly downturned, further reinforcing the impression of sadness. **As the video progresses**, his eyes appear to well up, **with slight moistness visible**, which is a clear indicator of **impending tears and emotional distress**. The overall expression remains **subdued and somber**, lacking any signs of anger, joy, or surprise, solidifying the interpretation of sadness.

Ground Truth Label: ANGER



Video-LLaMA 3: The person's mouth is **slightly open**, revealing their teeth, and their eyes are **focused intently on something off-camera**. The expression conveys a **sense of concern or contemplation**, suggesting they might be engaged in a **serious conversation** or deep in thought.

Qwen 2.5 VL: The facial expression in the video appears to be **neutral**. The person's **eyes are open and focused**, but there is no clear indication of anger, happiness, sadness, disgust, fear, or surprise. The **mouth is closed**, and the overall expression does not convey any strong emotion.


Video-LLaVA: The person in the video has a **serious facial expression**, with a **furrowed brow and a look of concentration**. This expression suggests that they are focused on something, possibly a task or a conversation. The person's facial expression is a reflection of their emotional state and the intensity of the situation they are in.

LLaVA-Video: The facial expression in the video is **neutral**. The person's **mouth is closed**, and there are no visible signs of emotional expression such as a smile or frown.

Emotion-LLaMA: In the image, a man with a beard and mustache is **looking directly at the camera**, his **eyes are narrowed**, and his **brows are furrowed**. This facial expression suggests that he is experiencing strong emotions, likely **anger or frustration** the combination of his **intense gaze and furrowed brows** indicates that he is focused on something specific, possibly a problem or issue that is causing him distress. **The context of the scene, which includes a man standing alone in a room, suggests that he may be feeling isolated or disconnected from others, further contributing to his emotional state**

Face-LLaVA (Ours): The subject's facial expression strongly suggests **anger**. His **eyebrows are furrowed**, creating **deep vertical lines between them**. His **eyes are wide and intense**, conveying a **sense of heightened arousal**. His **mouth is slightly open in a grimace**, and his **jaw is tense**, further emphasizing the **tension and frustration**. The overall expression is one of **intense displeasure and potential aggression**, all characteristic of **anger**.

Ground Truth Label: SURPRISE



Video-LLaMA 3: The **mouth is slightly open**, suggesting a **relaxed or neutral expression**. The lips are not tightly closed, indicating a **state of ease or mild engagement**.

Qwen 2.5 VL: The facial expression in the video appears to be **neutral**. The person's mouth is closed, and there are no visible signs of anger, happiness, sadness, disgust, fear, or surprise. **The eyes are looking slightly upwards**, which could **indicate a neutral or contemplative state**.

Video-LLaVA: The person in the video has a **neutral facial expression**, with their **eyes closed and their mouth open**. This expression could indicate that they are either **deep in thought or simply taking a moment to relax and breathe**. The person's facial expression is **not overly expressive**, but it does convey a sense of calmness and introspection.

LLaVA-Video: The facial expression in the video is **neutral**. The person's **mouth is closed**, and there are no visible signs of emotional expression such as a smile or frown.

Emotion-LLaMA: In the image, a young woman is looking directly at the camera with a **neutral expression**, her **eyes are focused on the lens**, and her **mouth is slightly open** the overall facial expression is one of concentration, suggesting that she is engaged in a task or activity the **lack of emotional cues and the focus on the camera's lens suggest that she is not expressing any strong emotions**, which could be interpreted as a sign of indifference or detachment from her surroundings the fact that she is not smiling or showing any other emotional expressions further supports this interpretation, as her facial expression appears to be neutral and unemotional

Face-LLaVA (Ours): The subject's **facial expression changes dramatically, indicating surprise**. **Initially**, her eyes are wide open, and her mouth is slightly parted, a classic sign of surprise. Her **eyebrows are slightly raised**, further emphasizing the **astonishment**. The **change in her expression is sudden and unexpected**, reinforcing the feeling of surprise. The overall effect is a clear visual representation of a **surprised reaction**.

Figure 18. Comparison of descriptions or reasoning obtained by Face-LLaVA with other baselines for facial expression recognition. **Blue text** indicates alignment with the ground truth and **red text** indicates wrong reasoning or hallucinations.



Figure 19. Comparison of descriptions or reasoning obtained by Face-LLaVA with other baselines for action unit detection. Blue text indicates alignment with the ground truth and red text indicates wrong reasoning or hallucinations. Notice that for AU detection, all the existing baselines hallucinate badly in getting the FACS action unit codes correct. However, our model is able to correctly capture both the FACS encoding and the correct activated AUs. Moreover, the left-most sample had a missing annotation for AU 17 (chin raiser) which is clearly visible in the image and Face-LLaVA correctly identifies the same.

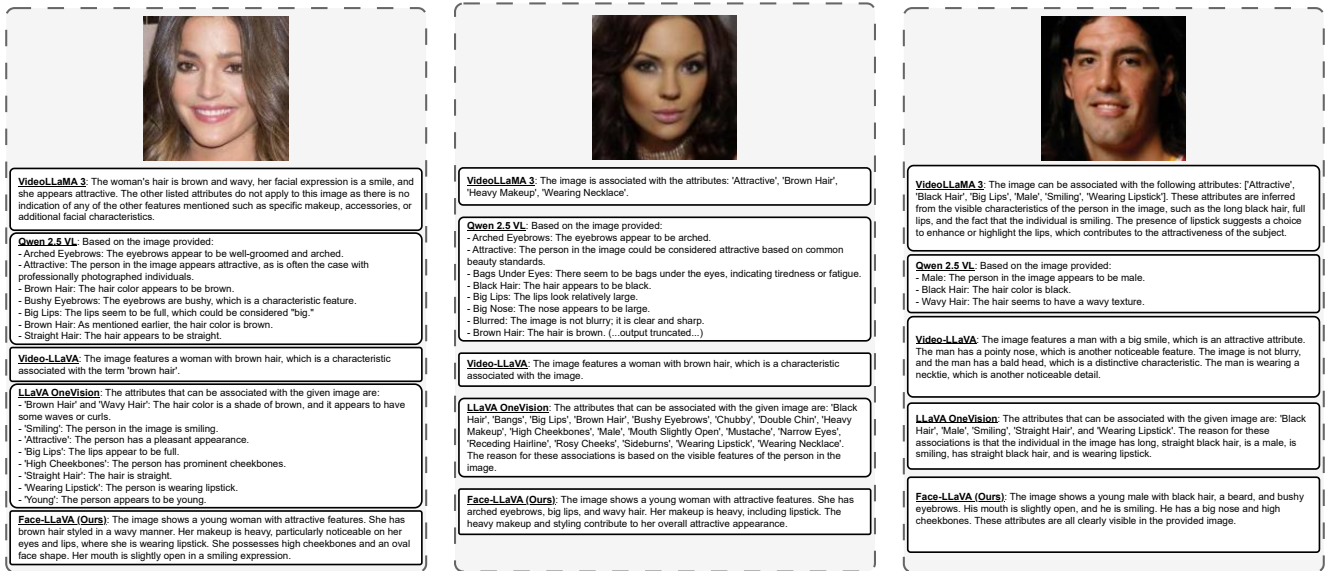


Figure 20. Comparison of descriptions or reasoning obtained by Face-LLaVA with other baselines for facial attribute detection. Note that for this task, we do not provide the ground truth label in the figure as the ground truth is clearly identifiable from the image. Also, note that for getting the baseline predictions for this task, we provide the list of possible attributes to the input prompt for the baselines to restrict their responses. Moreover, for computing the mean accuracy on CelebA [42] test set for this task for the baselines, we use a separate prompt where we ask the model to just detect the visible attributes and not describe them. This is done because our synonym matching does not work so accurately on formatted text (as shown above) generated by the baselines.




 <p>Ground Truth Age 4 years</p> <p>VideoLLaMA 3: The child in the image appears to be around 5 years old. This estimate is based on several visual cues: his size relative to the swing, the proportion of his features, and the general appearance of a typical 5-year-old child.</p> <p>Qwen 2.5 VL: The individual appears to be a young child, likely between 2 and 4 years old. The size of the head relative to the body, the facial features, and the overall appearance suggest this age range.</p> <p>Video-LLaVA: The person in the image is a young boy, likely around 3 to 5 years old.</p> <p>LLaVA OneVision: The person in the image appears to be a young child, likely around 3-5 years old. This estimation is based on their small stature, round face, and the overall appearance of a toddler.</p> <p>Face-LLaVA (Ours): 4 years old because the child exhibits facial features typical of that age range. The child's face is still quite round and cherubic, with soft features. The cheeks are full and rosy, and the overall expression is one of youthful innocence. The size and shape of the head also appear consistent with a preschool-aged child. While hair length can vary, the texture and style are not inconsistent with a young child of this age.</p>	 <p>Ground Truth Age 26 years</p> <p>VideoLLaMA 3: The person in the image appears to be a young adult, likely in his mid-20s. His facial features suggest he is not yet middle-aged, but has passed the typical teenage years. The overall appearance and demeanor indicate someone who is still in their early adult years.</p> <p>Qwen 2.5 VL: 25 years. The individual appears to be in their late twenties, based on facial features and general appearance.</p> <p>Video-LLaVA: The person in the image is described as a young man, which suggests that he is likely in his late teens or early twenties.</p> <p>LLaVA OneVision: The person in the image appears to be a young adult, likely in their late teens or early twenties. This estimation is based on the visible features such as the smooth skin and youthful appearance.</p> <p>Face-LLaVA (Ours): 26 years old is a reasonable estimate based on several observable facial features. The individual exhibits a level of facial maturity beyond that typically seen in someone younger than 25. The skin shows minimal signs of significant acne scarring or blemishes common in adolescence, suggesting a more developed skin texture. The overall facial structure, including the jawline and cheekbones, appears fully developed, indicating the completion of most adolescent growth spurts. The hairline is also consistent with someone in their mid-twenties, showing no significant signs of recession or thinning. While these are not definitive indicators, the combination of these features points towards an age range in the mid-twenties, with 26 being a plausible estimate.</p>	 <p>Ground Truth Age 58 years</p> <p>VideoLLaMA 3: The image shows a middle-aged man with gray hair and a mustache. Based on his facial features, particularly the full head of gray hair and the mature appearance, I estimate he's likely in his early 40s. Rounding to the nearest whole number, 20 is the closest approximation for this age range.</p> <p>Qwen 2.5 VL: The person appears to have a full head of hair, which often indicates they are past middle age. The presence of a mustache and the general facial features suggest that the individual is likely in their 60s or early 70s. Given these observations, an estimate of 65 years old seems reasonable.</p> <p>Video-LLaVA: The person in the image is described as an older man, which suggests that he is likely in his senior years. However, the exact age cannot be determined from the image.</p> <p>LLaVA OneVision: The person in the image appears to be an older adult, likely in their 60s or 70s. This estimation is based on visible signs of aging such as wrinkles and gray hair.</p> <p>Face-LLaVA (Ours): 58 years old is a reasonable estimate based on several observable facial features. The individual exhibits significant graying of the hair, which is a common indicator of aging. The presence of wrinkles around the eyes and forehead, along with some sagging of the skin, particularly around the jawline, further suggests a person in their late 50s. The overall texture of the skin also appears consistent with someone in this age range. While these are just visual estimations, the combination of these features points towards an age of approximately 58.</p>
--	---	---

Figure 21. Comparison of descriptions or reasoning obtained by Face-LLaVA with other baselines for age estimation. Blue text indicates alignment with the ground truth and red text indicates wrong reasoning or hallucinations. We can notice that the baselines provide minimal description for reasoning their predictions. Moreover, the reason is not based only on the facial features and has some inconsistencies (e.g. VideoLLaMA 3 [81] makes wrong age prediction even with correct reasoning for the right-most example.) In contrast to the baselines, Face-LLaVA is able to predict the age of the person in the image correctly with a detailed description specifically related to the facial features of the person in the image. Finally, it is important to note that we use a different prompt when we compute the performance of the baselines on traditional metrics (mean absolute error - refer Appendix F.3) as the baselines usually provide an age range in their descriptions and usual string parsing will have some inconsistencies due to that.




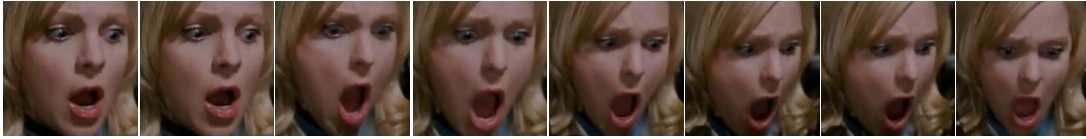
<p>Ground Truth Label: FAKE</p>  <p>VideoLLaMA 3: The video is manipulated. The facial features of the person in the video are altered, which indicates that it is a deepfake or a manipulated video.</p> <p>Qwen 2.5 VL: The image appears to be a still from a video, showing a person wearing glasses and a white shirt. The quality of the image suggests it might be from an older video source, possibly due to the graininess and color saturation. However, without additional context or frames from the video, it's difficult to definitively determine if the video has been manipulated. The image does not exhibit any obvious signs of digital manipulation such as unnatural lighting, inconsistent shadows, or pixelation that would typically indicate the use of deepfake technology. The overall appearance is consistent with a real-life recording.</p> <p>Video-LLaVA: The video shows a man with a beard and glasses, wearing a white shirt. He is making a face and appears to be in a state of distress. The man's facial expression and the way he is making a face suggest that the video is a deepfake. The video's visual cues, such as the man's facial expression and the way he is making a face, are inconsistent with the audio, which is not audible in the video. Additionally, the man's glasses appear to be distorted, which is another indication of a deepfake.</p> <p>LLaVA-Video: The video appears to be manipulated. The person's face is blurred, making it difficult to discern any facial features or expressions. The background is indistinct and dark, which further suggests that the focus is on the blurred face rather than providing context or setting. This lack of clarity and detail in the visual elements indicates that the video may have been altered or created using deepfake technology or other forgery tools.</p> <p>Face-LLaVA (Ours): Fake. The face in the video shows unnatural and inconsistent movements. The skin texture appears artificial and lacks the subtle variations and details seen in real human skin. The eyes, in particular, seem to lack natural blinking and movement, appearing somewhat static and lifeless. The overall facial expressions are stiff and unrealistic, lacking the fluidity and nuance of genuine human emotion.</p>	<p>Ground Truth Label: REAL</p>  <p>VideoLLaMA 3: The video is manipulated. The person's face is not real and looks like a computer-generated image.</p> <p>Qwen 2.5 VL: The video appears to be manipulated. The face in the image looks unnatural, with exaggerated features that do not align with typical human facial proportions. The lighting and shadows also seem inconsistent, which could indicate digital manipulation. Additionally, the overall quality of the image suggests it might have been generated or altered using deepfake technology. However, without more context or additional frames from the video, it's difficult to provide a definitive assessment.</p> <p>Video-LLaVA: The video features a woman with red lipstick and a nose piercing. She is wearing a necklace and has her eyes closed. The video is a deepfake, as indicated by the unnatural blinking and lip-sync mismatches. The lighting issues are also apparent, with the woman's eyes appearing to be closed, and the background is blurred. The motion artifacts are also noticeable, with the woman's head appearing to be jittery and her hair and glasses distorting.</p> <p>LLaVA-Video: The video appears to be manipulated. The close-up shots of the person's face are repeated multiple times with slight variations in the angle and position of the head, suggesting that the images have been edited or generated using a deepfake technique.</p> <p>Face-LLaVA (Ours): Real video. The face shows natural subtle movements like blinking, slight changes in expression, and lip movements. The skin texture appears natural with visible pores and minor imperfections, unlike the overly smooth and artificial look often seen in deepfakes. The video quality is consistent throughout, lacking the artifacts or inconsistencies that can indicate manipulation.</p>	<p>Ground Truth Label: FAKE</p>  <p>VideoLLaMA 3: The video is manipulated. The face of the woman in the video has been altered using deepfake technology.</p> <p>Qwen 2.5 VL: The video appears to be real. The facial expressions and movements seem natural, and there are no obvious signs of digital manipulation such as unnatural lighting, inconsistent shadows, or abrupt changes in texture that would typically indicate a manipulated image. The overall quality and consistency suggest it was recorded with a standard camera without any apparent post-processing alterations.</p> <p>Video-LLaVA: The video shows a woman with blonde hair and a smile on her face. She appears to be in a happy mood. The video is a deepfake, as indicated by the unnatural blinking and lip-sync mismatches. The lighting issues are also present, with the woman's eyes appearing to be reflecting light in an unnatural way. The motion artifacts are also noticeable, with the woman's head appearing to be jittery and her glasses distorting the image. Overall, the video is a deepfake, and the woman's facial expressions and movements are not natural.</p> <p>LLaVA-Video: The video appears to be manipulated. The person's face is blurred, making it difficult to discern any facial features or expressions. This suggests that the video has been altered or edited to obscure the individual's identity.</p> <p>Face-LLaVA (Ours): Fake video. The face in the video shows unnatural blurring and lack of fine details, especially around the eyes and mouth. The skin texture appears overly smooth and lacks the subtle variations in tone and texture seen in real-life videos. The overall movement of the face also seems slightly artificial and lacks the natural fluidity of human expression.</p>
---	--	---

Figure 22. Comparison of descriptions or reasoning obtained by Face-LLaVA with other baselines for deepfake detection. Blue text indicates alignment with the ground truth and red text indicates wrong reasoning or hallucinations. Other MLLMs hallucinate with their reasoning and provide descriptions that are not face-specific. Face-LLaVA on the other hand provides consistent descriptions that are face specific. Similar to attribute detection and age estimation, we use a different prompt for computing accuracy for the baselines on the FaceForensics++ [57] dataset for Tab. 5.

Ground Truth Label: Fear



Face-LLaVA: The subject's facial expression clearly indicates surprise. Initially, her eyes are wide open, and her mouth is slightly parted, suggesting a state of alertness or anticipation. However, as the video progresses, her mouth opens much wider in an 'O' shape, and her eyebrows are slightly raised. This combination of wide eyes, an open mouth, and slightly raised eyebrows is a classic indicator of surprise. The rapid change in her facial expression from a state of mild alertness to a clear expression of astonishment further strengthens the interpretation of the emotion as surprise.

Ground Truth Label: Sadness



Face-LLaVA: The subject's facial expression remains relatively static throughout the video. There are no significant changes in brow furrow, lip corners, or eye widening that would typically indicate emotions like happiness, sadness, anger, or surprise. The mouth is slightly open, which could be interpreted as slight surprise or concern, but it's not intense enough to definitively classify the emotion as anything other than neutral. The overall expression is one of mild contemplation or perhaps slight apprehension, but lacks the intensity or distinct features associated with clearly defined emotions.

Ground Truth Label: Neutral



Face-LLaVA: The subject's facial expression conveys sadness through several cues. His eyebrows are slightly furrowed, indicating a level of distress or worry. His gaze is downcast, avoiding direct eye contact, which is often associated with feelings of sadness or dejection. His mouth is slightly downturned, forming a subtle frown, further reinforcing the overall impression of sadness. The overall expression is one of quiet contemplation and sorrow, rather than an outburst of intense emotion. There is a stillness to his face, lacking the dynamism of other emotions.

Ground Truth Label: Fear



Face-LLaVA: The subject's facial expression conveys sadness primarily through her eyes and mouth. Her eyes appear downcast and slightly watery, lacking their usual brightness. This suggests a feeling of dejection or hopelessness. Her mouth is slightly downturned, forming a subtle frown, further reinforcing the sadness. While the presence of wounds on her face adds to the overall bleakness of the scene, the primary indicator of sadness is the subtle yet noticeable downturn of her mouth and the lack of sparkle in her eyes. The expression is not overtly dramatic, but rather a quiet, subdued sadness.

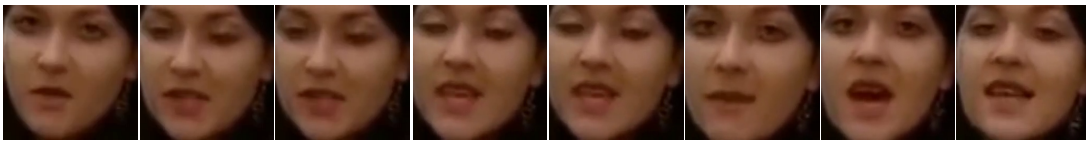
Figure 23. Failure cases for facial expression recognition task on some samples of DFEW [22]. In the samples above, expressions labeled as ground truth *fear* are often misclassified as *sadness* or *surprise*. Closer inspection of the videos reveals that these instances indeed exhibit mixed emotions. Additionally, ground truth labels are assigned based on the full scene, incorporating background context and audio, whereas Face-LLaVA makes predictions solely from the face-cropped video.

Ground Truth Label: Fake



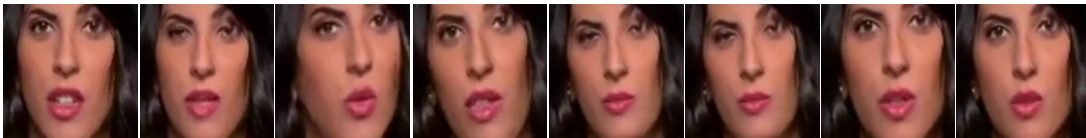
Face-LLaVA: Real video. The face shows natural skin texture with pores, subtle imperfections, and realistic variations in lighting and shadow across the face. The slight movements of the eyes and mouth are natural and fluid, lacking the stiffness often seen in deepfakes. The video quality is consistent with older recordings, showing some compression artifacts but no obvious signs of digital manipulation or splicing.

Ground Truth Label: Fake



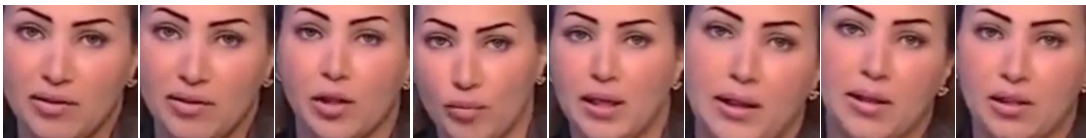
Face-LLaVA: Real video. The video shows a close-up of a woman's face. The face displays natural imperfections, including subtle skin texture, slight asymmetry, and realistic lip and eye movements. The lighting appears consistent and natural, without any obvious signs of digital manipulation or artificial enhancements. The video quality is consistent with older recordings, showing some grain and compression artifacts, which are typical of non-manipulated footage.

Ground Truth Label: Fake



Face-LLaVA: Real video. The face shows natural subtle movements like slight changes in expression and lip movements that are consistent with a real person speaking. The skin texture appears natural with visible pores and minor imperfections, unlike the smooth, flawless skin often seen in manipulated videos. The video quality is consistent throughout, lacking any jarring transitions or inconsistencies that might suggest editing or manipulation.

Ground Truth Label: Real



Face-LLaVA: Fake. Real human faces have subtle variations in texture and lighting that are difficult to perfectly replicate. In this video, the face appears overly smooth and lacks the natural imperfections and subtle changes in skin tone and texture that one would expect in a real video. The eyebrows appear unnaturally uniform and sharply defined, lacking the natural variations in hair thickness and direction. The overall appearance of the face is too perfect and lacks the realistic imperfections found in real-life videos.

Figure 24. Failure cases for deepfake detection task on some samples of FaceForensics++ [57]. In the first and third samples above, determining whether the videos are manipulated is challenging even for human beings, as they were altered using a face re-enactment technique (NeuralTextures). In the last example, the model mistakenly classifies a real video as fake, attributing its decision to the smoothness of the skin and makeup around the eyes, interpreting the face as “too perfect” to be real.

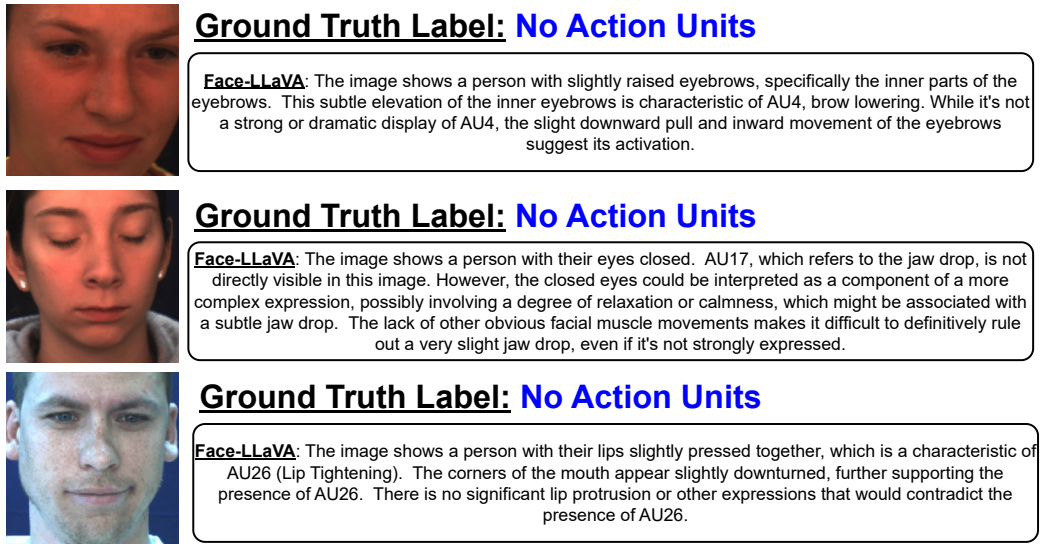


Figure 25. Failure cases for action unit detection task on some samples of DISFA [46]. Our model fails mostly on the cases when the ground truth sample does not have any action units activated.

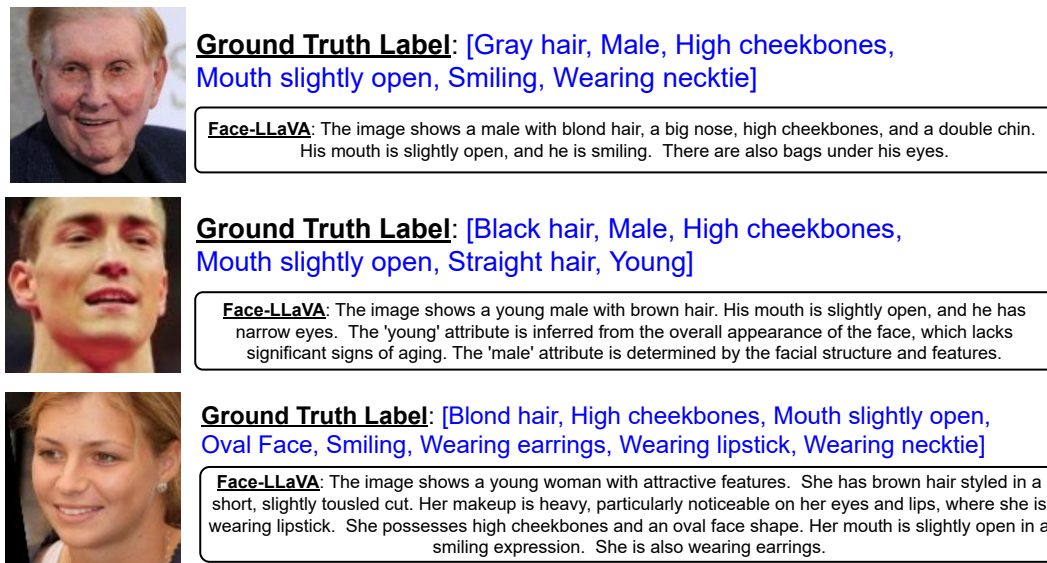


Figure 26. Failure cases for facial attribute detection task on some samples of CelebA [42]. In the above examples, while the model's predictions slightly differ from the ground truth, they remain consistent with the visual content of the image, suggesting potential imperfections in the dataset annotations of CelebA.



Ground Truth Age: 11 years

Face-LLaVA: 16 years old because the individual exhibits facial features consistent with that age group. The person's facial structure shows a blend of youthful and developing characteristics. The skin appears relatively clear with minimal signs of significant acne scarring or deep wrinkles, common in older individuals. The overall shape of the face and the proportions of the features, such as the nose and jawline, suggest a person in the mid-teens rather than a younger or older age. The hairline and hair texture also appear typical for a 16-year-old.



Ground Truth Age: 12 years

Face-LLaVA: 24 years old is a reasonable estimate based on several observable features. The individual's facial features, particularly the development of the jawline and cheekbones, suggest an age beyond the early twenties. The skin exhibits a texture and tone consistent with someone in their mid-twenties, showing minimal signs of significant aging or acne scarring often associated with younger ages. Furthermore, the overall facial structure and expression convey a maturity level that aligns with the 24-year-old age range. It's important to note that this is an estimation based on visual cues and may not be perfectly accurate.



Ground Truth Age: 80 years

Face-LLaVA: 65 years old is a reasonable estimate based on several observable features. The individual's extensive network of wrinkles around the eyes and forehead, particularly the crow's feet, are consistent with significant sun exposure and the natural aging process over many years. The presence of significant sagging skin on the face, particularly noticeable around the jawline and cheeks, also points towards an older age. The individual's hair is largely white or gray, which is a common indicator of aging. The overall texture of the skin appears thinner and less elastic than that of a younger person. While these are just indicators and not definitive proof, the combination of these features strongly suggests an age in the mid-60s.

Figure 27. Failure cases for age estimation task on some samples of UTKFace [87]. Except for the middle sample, the error in prediction for the other two samples are acceptable and even for humans it is hard to judge the age.